Unravelling the role of thyroid hormones in seasonal neuroplasticity in European Starlings (Sturnus vulgaris)

Orije Jasmien[1,2], Raymaekers Sander R.[3], Gaurav Majumadar[1], De Groof Geert[1], Jonckers Elisabeth[1,2], Ball Gregory F.[4], Marleen Verhoye[1,2], Darras Veerle M.[3], Van der Linden Annemie[1,2]

1 Bio-Imaging Lab, University of Antwerp, Belgium

2 µNEURO Research Centre of Excellence, University of Antwerp, Belgium

3 Laboratory of Comparative Endocrinology, Biology Department, KU Leuven, Belgium

4 College of Behavioral and Social Science, University of Maryland, USA

11   1.   # Abstract:

12   Thyroid hormones clearly play a role in the seasonal regulation of reproduction, but any role they

13   might play in song behavior and the associated seasonal neuroplasticity in songbirds remains to be

14   elucidated. To pursue this question, we first established seasonal patterns in the expression of thyroid

15   hormone regulating genes in male European starlings employing *in situ* hybridization methods.

16   Thyroid hormone transporter *LAT1* expression in the song nucleus HVC was elevated during the

17   photosensitive phase, pointing towards an active role of thyroid hormones during this window of

18   possible neuroplasticity. In contrast *DIO3* expression was high in HVC during the photostimulated

19   phase, limiting the possible effect of thyroid hormones to maintain song stability during the breeding

20   season. Next, we studied the effect of hypothyroidism on song behavior and neuroplasticity using *in*

21   *vivo* MRI. Hypothyroidism inhibited the photostimulation-induced increase in testosterone,

22   confirming the role of thyroid hormones in activating the hypothalamic–pituitary–gonadal (HPG) axis.

23   Surprisingly, apart from the myelination of several tracts during the photostimulated phase, most

24   neuroplasticity related to song production was unaffected by hypothyroidism. Remarkably, T3 plasma

25   concentrations were negatively correlated to the microstructural changes in several song control

26   nuclei. Potentially, a global reduction of circulating thyroid hormones during the photosensitive period

27   is necessary to lift the brake imposed by the photorefractory period, whereas local fine-tuning of

28   thyroid hormone concentrations through LAT1 could activate underlying neuroplasticity mechanisms.

29   Given the complexity of thyroid hormone effects, this study is a steppingstone to disentangle the

30   influence of thyroid hormones on seasonal neuroplasticity.

2. Introduction:

Seasonal changes in steroid hormone concentrations such as testosterone play a central role in the regulation of song behavior and the associated neuroplasticity in seasonal songbirds (Balthazart, Charlier et al. 2010). For example, testosterone acting in the pre-optic area can increase the motivation to sing, resulting in activity-induced neuroplasticity, including increased forebrain song control nuclei volume (Alward, Balthazart et al. 2013) and stronger connections between the song control nuclei (Orije, Cardon et al. 2020). In several songbird species, testosterone is known to be necessary for the crystallization of song (Marler, Peters et al. 1988, Korsia and Bottjer 1991, Williams, Connor et al. 2003), while castration increases syllable's entropy and decreases the song similarity and stereotypy (Wang, Liao et al. 2014). Male canaries sing a stable song during the breeding season, when testosterone levels are high. As canaries become photorefractory in fall, their testosterone levels decrease and their song becomes plastic again (Nottebohm, Nottebohm et al. 1987, Voigt and Leitner 2008, Alward, Mayes et al. 2014). Female canaries also produce song, when they are implanted with testosterone, their song rate increases and their song becomes stable. Female starlings implanted with testosterone show the same behavioral changes. Furthermore, when the testosterone implant is removed, song control nuclei rapidly decrease in volume (Orije, Cardon et al. 2020).

These studies demonstrate that testosterone can play a key role in stimulating songbirds of various species to sing at higher rates and to crystalize or stabilize their song, and that these behavioral changes are associated with structural changes in their song control system. The presence of aromatase, androgen and estrogen receptors in several song control nuclei (**Figure 10**) is consistent with the notion that testosterone can act directing in these key song control nuclei to induce changes in morphology and physiology. However, several studies have shown that even in absence or presences of very low concentrations of gonadal testosterone seasonal neuroplasticity can still occur, indicating that there are other factors that regulate or influence seasonal neuroplasticity (Smith, Brenowitz et al. 1997, Bentley, Van't Hof et al. 1999, Dawson, King et al. 2001). One of the candidate factors that might regulate seasonal plasticity in brain and behavior are thyroid hormones. The avian thyroid gland produces thyroxine (T4) as well as a small amount of triiodothyronine (T3), which are both released into the bloodstream. Thyroid hormone activity is subsequently regulated at multiple levels. Several thyroid hormone transporters, including monocarboxylate transporters (MCT8 and MCT10), Na-independent organic anion transporting polypeptide 1C1 (OATP1C1), and L-type amino acid transporter 1 (LAT1) facilitate transport of T3 and T4 across the cell membrane (Heuer and Visser

62   2009). Once in the cell, the activity of thyroid hormones can be locally adjusted by deiodinases.

63   Deiodinase 2 (DIO2) converts the prohormone T4 into its more bioactive form T3. Contrary, deiodinase

64   3 (DIO3) inactivates T4 and T3 to reverse T3 (rT3) and T2 respectively (Gereben, Zavacki et al. 2008).

65   Thyroid hormones mostly operate by modulating gene expression as a result of binding of T3 to

66   nuclear thyroid hormone receptors alpha or beta (THRA or THRB). These receptors associate with

67   thyroid hormone response elements in the promotor region and induce or repress gene expression,

68   depending on the gene.

69   Thyroid hormone levels change seasonally and are known to play a role in reproductive maturation

70   and maintaining the photorefractory state in seasonally breeding birds (Bentley, Goldsmith et al. 1997,

71   Bentley, Dawson et al. 2000). They closely interact with the hypothalamus-pituitary-gonadal (HPG)

72   axis. One of the first things to change after exposure to a single long day of Japanese quail is the local

73   upregulation of thyroid stimulating hormone (TSH) and DIO2 and downregulation of DIO3 in the pars

74   tuberalis of the pituitary gland. This results in a local increase in T3 in the mediobasal hypothalamus,

75   which causes gonadotropin releasing hormone (GnRH) release from morphologically changed GnRH

76   nerve terminals and activates the rest of the HPG-axis (Yoshimura, Yasuo et al. 2003, Watanabe,

77   Yamamura et al. 2007, Nakao, Ono et al. 2008). So far this link between thyroid hormones and gonadal

78   steroid hormone production was not confirmed in starlings (Bentley, Tucker et al. 2013). Furthermore,

79   thyroid hormones are known to play a role during neuronal development and are suggested to

80   influence critical period learning (Bernal 2000, Yamaguchi, Aoki et al. 2012, Batista and Hensch 2019).

81   However, the exact role of thyroid hormones in seasonal neuroplasticity in song and the song system

82   has not been investigated yet.

83   We hypothesize that thyroid hormones contribute to the seasonal neuroplasticity related to song

84   behavior. If thyroid hormones are indeed able to actively influence seasonal neuroplasticity, we expect

85   in the first place expression of thyroid hormone receptors, transporters and deiodinases in the song

86   bird brain and more specifically in the song control system. The first report describing a role of thyroid

87   hormone regulating genes during development of the song control system and song learning in the

88   zebra finch brain came from our coauthors (Raymaekers, Verbeure et al. 2017). They showed that

89   DIO2 and LAT1 expression in several song control nuclei remained high during the sensory and

90   sensorimotor phase of song learning in male zebra finches, suggesting that thyroid hormones are key

91   players in this process. In line with the role of thyroid hormones in song development in zebra finches,

92   we expected that the expression of thyroid hormone regulating genes could change seasonally in

93   starlings and have differential effects in regulating song and neuroplasticity across the seasons. Once

94   we had established the spatial and temporal expression patterns of thyroid hormone regulating genes

95 (and thyroid hormone plasma levels) during different photoperiods, we induced hypothyroidism
96 during the photosensitive stage to investigate the impact on seasonal neuroplasticity and song
97 production (**Figure 1**).

98 In short, this study aimed to answer the following questions: (1) Are thyroid hormone regulatory genes
99 expressed in the song control system of male starlings? (2) Does their expression change seasonally?
100 (3) Does thyroid hormone manipulation affect the HPG-axis just like in Japanese quail? (4) Does thyroid
101 hormone deprivation affect seasonal neuroplasticity and song behavior in male starlings?

102 We tried to answer the last question by inducing thyroid hormone deprivation at the onset of the
103 photosensitive stage while using *in vivo* MRI to monitor neuroplasticity in starlings as they passed
104 through different photoperiodic states. In a previous MRI study, we showed that seasonally increased
105 neuroplasticity starts during the photosensitive period, which acts as a sensitive window for
106 multisensory neuroplasticity as it shows involvement of the song control, visual and auditory system
107 and even the cerebellum (Orije, Cardon et al. 2021). Furthermore, *in vivo* MRI is a powerful tool to
108 study neural substrate changes associated with singing behavior or hormonal changes (Hamaide,
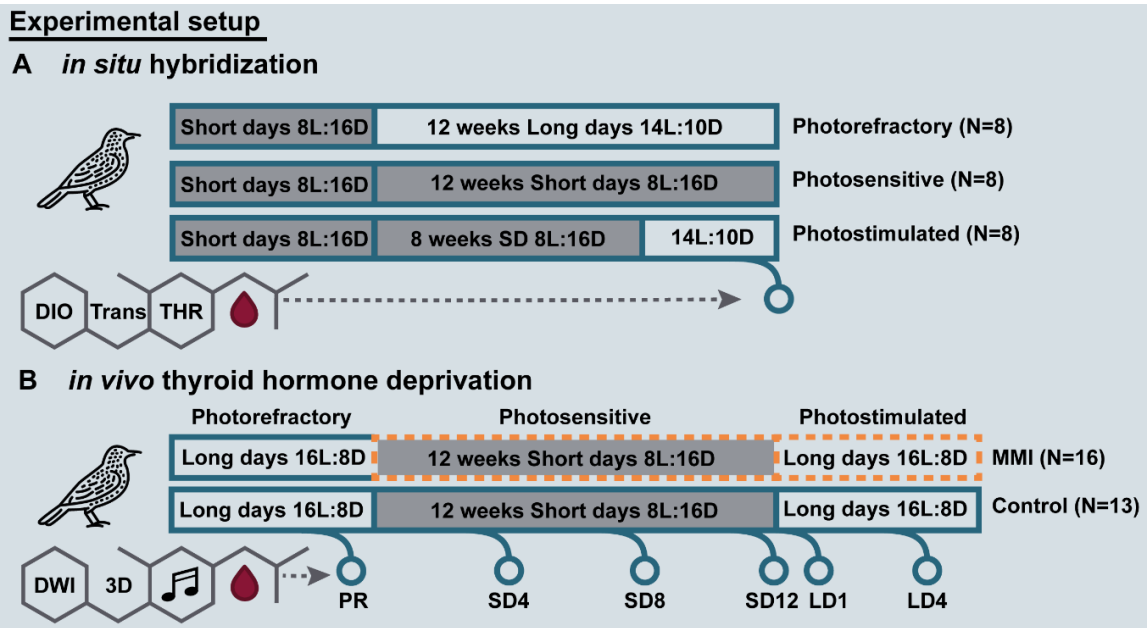109 Lukacova et al. 2020, Orije, Cardon et al. 2020, Orije, Cardon et al. 2021).

110
111 **Figure 1: Overview experimental setup of in situ hybridization (A) and in vivo thyroid hormone deprivation**
112 **(B) study.** For *in situ* hybridization, all birds were photosensitive after being on a short day photoperiod. These
113 birds were divided into three groups with different photoperiodic manipulation: 12 weeks of long days to induce
114 the photorefractory state, 12 weeks of short days to maintain photosensitive state, 8 weeks of short days
115 followed by 4 weeks of long days to induce photostimulated state. For each photoperiod we analyzed different
116 thyroid hormone regulators: deiodinases (DIO), thyroid hormone transporters (Trans), and thyroid hormone
117 receptors (THR). For the in vivo manipulation study, we monitored individual starlings as they went through
118 different photoperiods sequentially and diffusion weighted images (DWI) and 3D scans were acquired at the
119 indicated time points. Short days (SD) are indicated by a grey box. Methimazole (MMI) treatment is indicated by
120 an orange dotted line.

3.   Results

3.1 Thyroid hormone regulators in the song control system: *in situ* hybridization

To understand fully the role and regulation of thyroid hormone action in seasonal neuroplasticity in male starlings, we performed ISH for mRNA of all known major thyroid hormone regulators. Of these thyroid hormone regulators *DIO2, MCT8, MCT10* and *OATP1C1* showed no visible expression in any of the photoperiods in any of the song nuclei nor in the rest of the telencephalon.

Of the main thyroid hormone activating and inactivating enzymes DIO2 and DIO3, only *DIO3* expression was detected in the HVC and varied over the different photoperiods ($F_{(2, 18)}$=9.69 p=0.0014). Photorefractory and photosensitive birds showed little to no *DIO3+* cells, whereas *DIO3* expression was much higher after 4 weeks of photostimulation (**Figure 2A and Figure 3 A-C**).

In contrast to the other thyroid hormone transporters, *LAT1* exhibited a strong expression in HVC in all three photoperiods ($F_{(2, 18)}$= 4.10, p=0.0342) (**Figure 3 D-F**). *Post hoc* Bonferroni test showed that the *LAT1* expression in the HVC in the photosensitive state was significantly higher than in the photostimulated phase (**Figure 2B**). Furthermore, there was a low, widespread expression of LAT1 in the upper layers of the pallium both rostrally and caudally and a low expression in the arcopallium including RA. No expression was observed in other song control nuclei.

Finally, we examined the expression pattern of thyroid hormone receptors. *THRA* showed a clear and widespread expression throughout the entire pallium including HVC, RA and LMAN, whereas no expression was detected in the striatum, including Area X (representative image shown in **Figure 3 G-I**). In general, there was no variation in *THRA* expression over the different photoperiods. Furthermore, the *THRA* expression was not specific for the song control nuclei, since similar density and intensity of *THRA* expression was found in the surroundings of HVC, RA and LMAN. *THRB* expression was much lower compared to *THRA* and was only found in upper layers of the pallium and caudal arcopallium but not detected in the RA or any other song control nucleus (**Figure 3 J-L**).

The widespread expression of *THRA* makes it possible for seasonal changes in T4 and T3 to affect several song control nuclei, except striatal regions like Area X. Active seasonal changes in thyroid hormone regulating genes (*DIO3* and *LAT1*) are confined to the HVC, as the central regulator of other

149   song control nuclei it is connected to. This suggests that the intracellular concentration of thyroid

150   hormones is actively controlled at the level of HVC, and could play a role in seasonal song behavior.

151

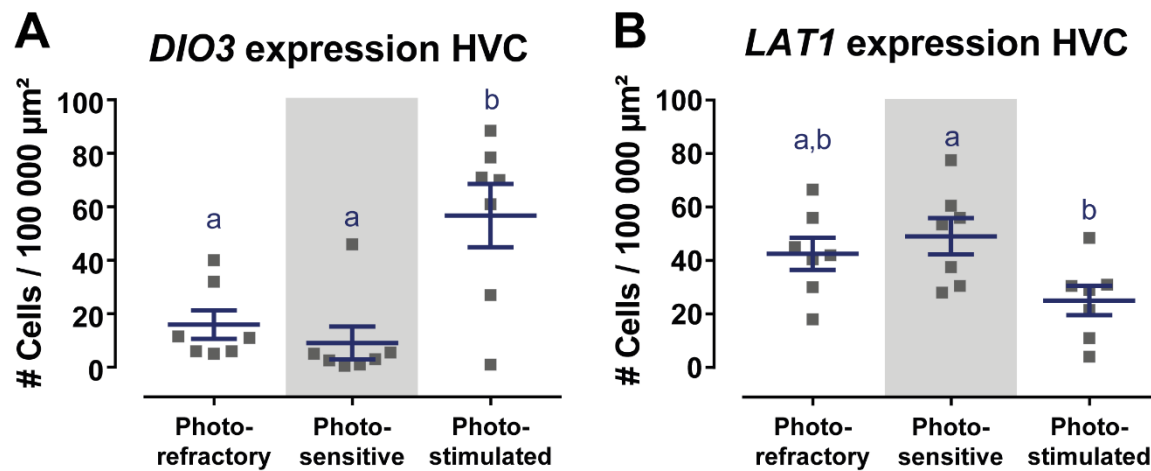**Figure 2: Overview of DIO3 (A) and LAT1 (B) expression in the HVC in the photorefractory, photosensitive and photostimulated phase.** Dots represent the average number of DIO3+ and LAT1+ cells per individual bird. Horizontal bars represent the average with standard error of the mean error bars (n=7). The grey area indicates the photosensitive phase. Different letters denote significant differences by comparison with each other in post-hoc t-tests with p < 0.05 (multiple comparison correction with Dunn's post hoc tests for DIO3 and Bonferroni correction for LAT1). If two time points share a common letter, DIO3 or LAT1 expression are not significantly different from each other.
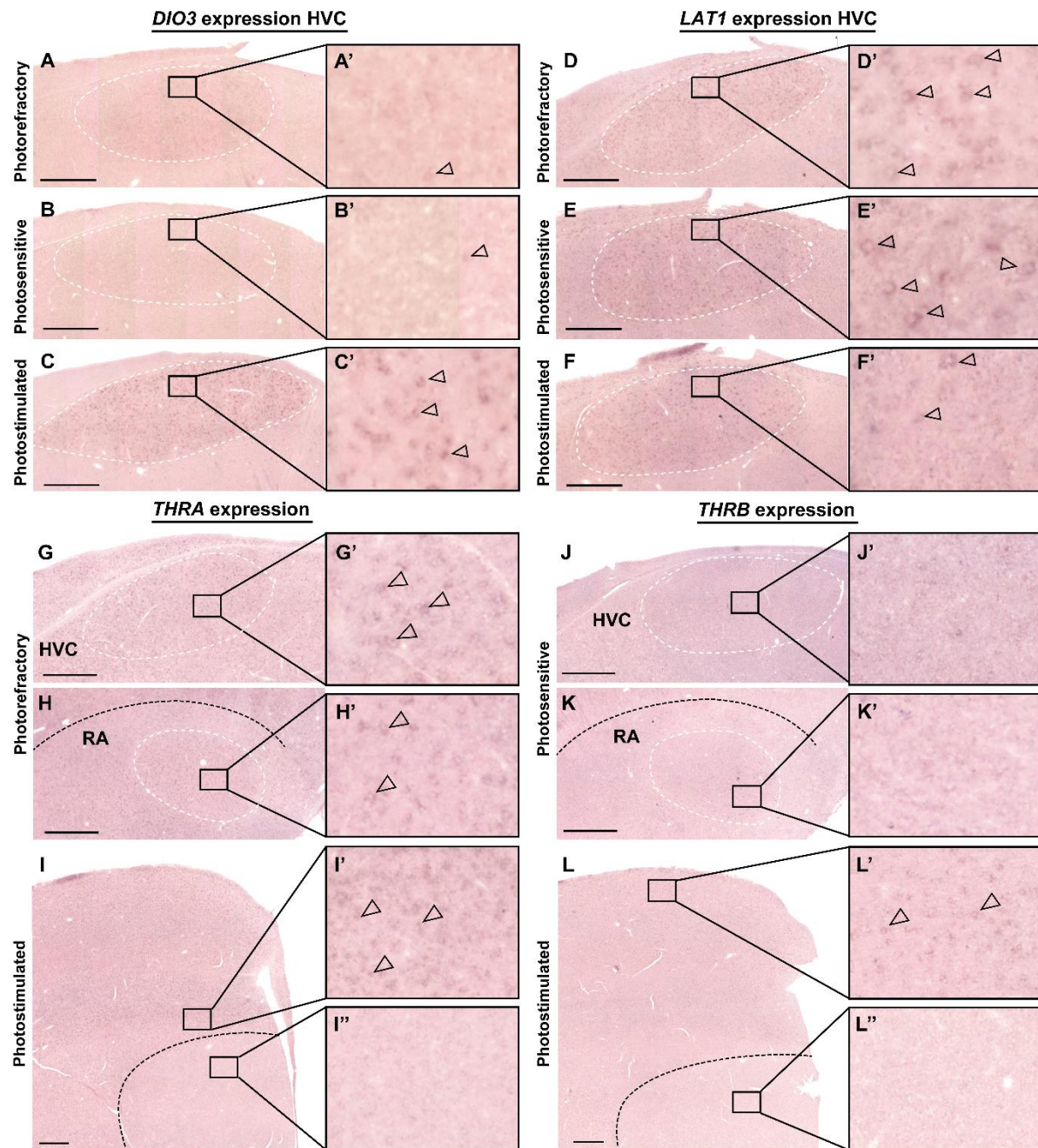
159

Figure 3: Representative images of *DIO3* (A-C), *LAT 1* (D-F), *THRA* (G-I), *THRB* (J-L) mRNA expression in the starling brain. *DIO3* and *LAT1* mRNA expression changes seasonally over the photorefractory (A, D), photosensitive (B, E) and photostimulated phase (C, F). *THRA* and *THRB* mRNA expression remain unchanged during the different seasons in caudal telencephalon (G, H, J, K) at the level of HVC (G, J) and RA (H, K) and in the rostral telencephalon (I, L) at the level of LMAN (I'), pallium (L') and Area X (I'', L''). The inserts indicate the location of the close-ups (A'-L'). The borders of HVC and RA are designated by white dashed lines. Black dashed line indicates the border between nidopallium and arcopallium in (H, K) and the border between striatum and pallium in (I, L). Empty arrowheads designate examples of DIO3+, LAT1+ and THRA+ cells respectively. Scale bar in overview pictures are 500µm.

169   3.1.1 Validation of ISH cell counting

170   To evaluate the validity of the cell count method used for the *DIO3* and *LAT1* ISH, 10 random sections
171   of both ISHs were analyzed using the semi-quantitative manner of 'stained surface fraction'. The
172   correlation between both methods measuring expression (stained surface fraction values and original
173   count value) was examined. The r² was 0.944 for the *DIO3* ISH and 0.924 for the *LAT1* ISH.

174   Furthermore, we investigated whether a change in cell density in the HVC across seasons could result
175   in changes in *DIO3+* and *LAT1+* cell counts, by performing a Nissl staining on sections from each
176   photoperiodic treatment in 3 birds. Cells stained by cresyl violet were counted in HVC, but numbers
177   showed no variation over time (F(2, 20)=0.44, p=0.649) (Figure 3 – figure supplement 1).

178   3.2 **Hypothyroidism by MMI treatment affects circulating thyroid**
179   **hormones (T3 and T4) and testosterone concentrations.**

180   The aim of the MMI treatment was to inhibit thyroid hormone production in order to establish how
181   hypothyroidism affects seasonal neuroplasticity. To confirm the effectiveness of this treatment, we
182   took blood samples at each time point to monitor plasma levels of T3 and T4. At the baseline
183   photorefractory time point there was no difference in circulating thyroid hormone concentrations
184   between groups. MMI treatment was successful in reducing both T3 and T4 to a minimum at 4 weeks
185   after starting MMI treatment upon the switch to short days (**Figure 4 A, B**). Thyroid hormone levels
186   remained low for the rest of the experiment. In the control group T4 and T3 significantly decreased
187   during the photosensitive period compared to the photorefractory period. After switching back to
188   long days, T4 concentrations significantly increased again to levels comparable to the photorefractory
189   period, while T3 concentrations remained low.

190   Additionally, we monitored circulating testosterone concentrations to determine how photoperiod
191   and MMI treatment affect the HPG-axis. While the HPG-axis matured in the control group as shown
192   by the elevated circulating testosterone levels during the photostimulated phase, circulating
193   testosterone level remained low throughout the different photoperiods in the MMI-treated group
194   (**Figure 4 C**). However, the beak color of MMI-treated birds turned yellow at the end of the
195   photosensitive phase and in the photostimulated phase just like in the control group (**Figure 4 D**). Beak
196   color does not directly represent the amount of circulating testosterone, but rather indicates that
197   testosterone is present in circulation, even when in low doses below the sensitivity limit of the RIA
198   assay (Ball and Wingfield 1987, Wingfield and Silverin 2002). Overall, MMI treatment does not only

199   decrease thyroid hormone but also testosterone plasma concentrations. However, testosterone was

200   not totally eliminated, as can happen with castration, as indicated by the beak color changing to yellow

201   in the MMI treated birds. Overall these data indicate that thyroid hormones indeed influence HPG-

202   axis physiology in starlings as hypothesized previously based on work in other species (Yoshimura
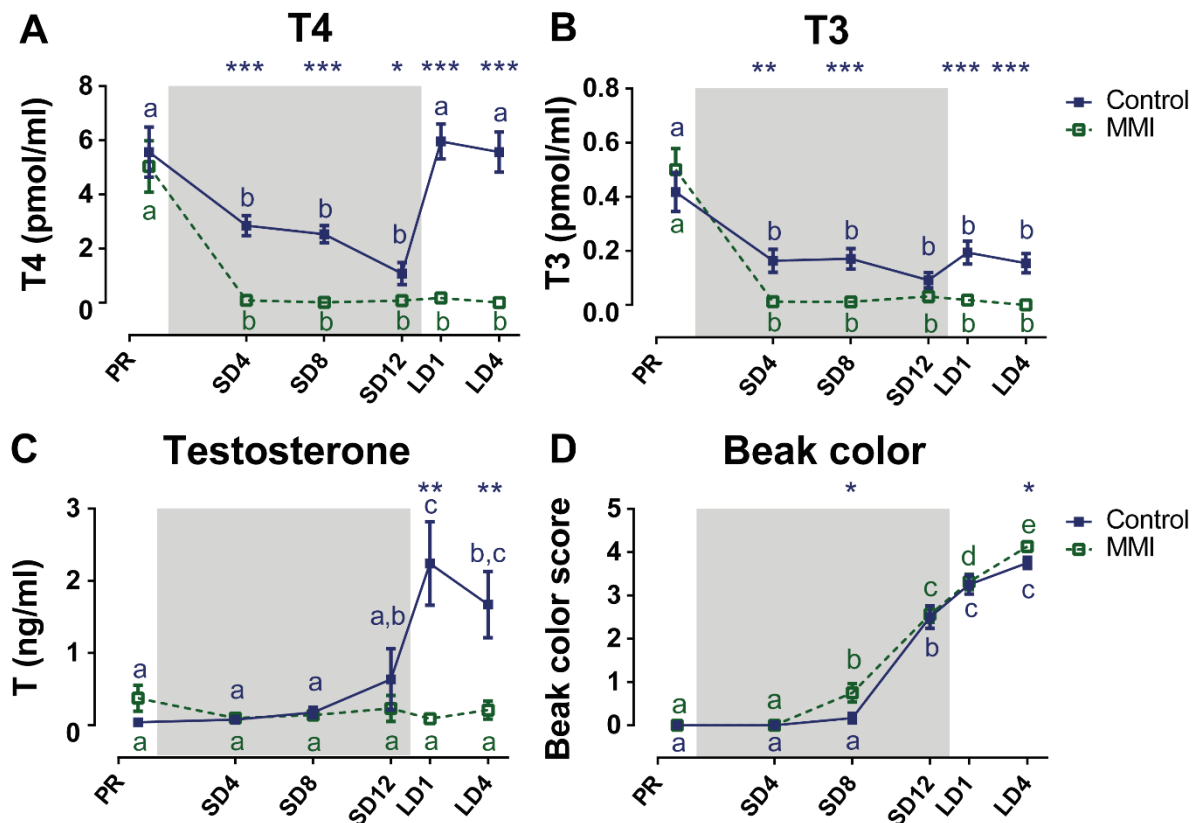
203   2013).

204

205   **Figure 4: Overview of the seasonal changes in plasma levels of thyroid hormones T4 (A), T3 (B), testosterone**
206   **(C) and beak color (D) in control and MMI-treated starlings**. Solid and dashed lines represent the group average
207   of control and MMI-treated starlings respectively with standard errors of the mean error bars. The grey area
208   indicates the photosensitive period of short days (8L:16D). Different letters denote significant differences by
209   comparison with each other in post-hoc t-tests with p < 0.05 (Tukey's HSD correction for multiple comparisons)
210   comparing the different time points to each other. If two time points share a common letter, the thyroid
211   hormone or testosterone levels are not significantly different from each other.

3.3 **Hypothyroidism by MMI treatment differentially affects song rate and song bout length**

We also investigated how MMI treatment affects the change in song behavior over different photoperiods. Both control and MMI-treated male starlings sang a longer song bout during the photostimulated phase compared to the photosensitive phase, but MMI-treated starlings further increased their song bout length during the photostimulated phase from 35.26±0.62 seconds at LD1 to 39.36±0.71 seconds at LD4 (**Figure 5**). Furthermore, song bout length was within-subjects positively correlated with the testosterone concentration in the control group (rmcorr=0.572, p=0.0054). Since testosterone plasma concentration in the MMI-treated group did not change over different seasons, it was not correlated to song bout length. However, beak color, which is a sensitive indicator of the presence or absence of circulating testosterone, did positively correlate to song bout length in both groups (control: rmcorr=0.592, p=0.0015; MMI: rmcorr=0.4136, p=0.0287). Unlike the song bout length, the song rate did not change over time nor did it correlate to hormone levels in either group. However, the untreated male starlings had a higher song rate compared to MMI-treated starlings after 4 weeks of photostimulation.
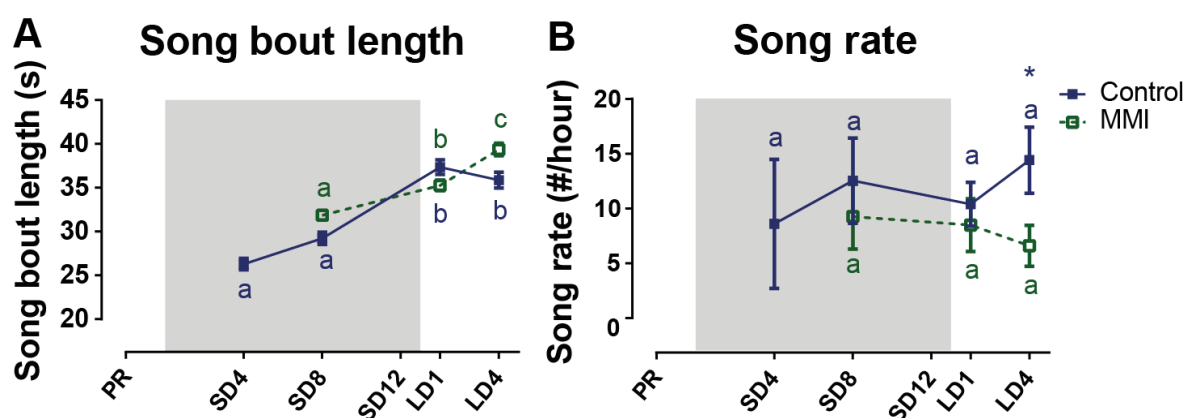

Figure 5: Overview of the seasonal changes in song bout length (A) and song rate (B) in control and MMI-treated starlings. Solid and dashed lines represent the group average of control and MMI-treated starlings respectively with standard errors of the mean error bars. The grey area indicates the photosensitive period of short days (8L:16D). Different letters denote significant differences by comparison with each other in post-hoc t-tests with p < 0.05 (Tukey's HSD correction for multiple comparisons) comparing the different time points to each other. If two time points share a common letter, the song bout length and song rate are not significantly different from each other.

3.4 Effect of hypothyroidism on seasonal neuroplasticity: a longitudinal DTI study

In order to determine whether thyroid hormone deprivation affects neuroplasticity, we used *in vivo* DWI to monitor structural neuroplasticity changes within the starling brain, using the same method as Orije, Cardon et al. (2021). This method measures several diffusion parameters that can provide information on microstructural changes related to structure and spatial organization of neuronal cells and myelin (Orije, Cardon et al. 2020, Orije, Cardon et al. 2021). A voxel based factorial analysis was performed to establish the general fractional anisotropy changes over time and if this differed between both experimental groups, it was indicated by a significant interaction. The results are summarized in **Figure 6, Figure 7 and Table 1.** From each significant cluster, we extracted the mean fractional anisotropy values and plotted them over time to determine the profile of temporal changes in fractional anisotropy (**Figure 6, Figure 7 B, D**). Additionally, we extracted other diffusion parameters (mean, axial and radial diffusivity) and fixel-based measures from these ROIs to provide more insight into the basis of the fractional anisotropy change (**Figure 6- figure supplements 1-2, Figure 7 - figure supplements 1-2**). For the statistical analysis of the extracted parameters, we used linear mixed model analysis with Tukey's Honest Significant Difference (HSD) as multiple comparison correction during *post hoc* statistics.

Overall most neuroplasticity changes looked similar in both groups. In line with the prior longitudinal MRI study (Orije, Cardon et al. 2021), the fractional anisotropy value of several parts of the song motor pathway, anterior forebrain pathway but also visual system and molecular layer of the cerebellum increase gradually over time, starting during the photosensitive period. The MMI-treated group had higher FA values in the molecular layer of the cerebellum at several time points, including the first time point. Since the difference was already present at the start of the experiment, before the start of MMI treatment, it most probably reflects unintended sample variation between groups. Despite this unintended group difference, both groups experienced a similar increase in FA over time.

Only a small part of the left OM showed a significant interaction between time and group. The control group peaked in fractional anisotropy at SD12, whereas the MMI-treated group reached a maximum at LD1. *Post hoc* linear mixed model analysis revealed more subtle interactions over time in the different groups. In the rostral part of the left Area X surroundings, the control group had a decrease in fractional anisotropy at LD4, whereas in the MMI group fractional anisotropy remained constant. In the MMI group fractional anisotropy values in LMAN significantly increased at SD4, whereas fractional anisotropy values in the control group only increased at the end of the photosensitive period. Most

268   interestingly, several tracts including the OM, tFA and optic tract have similar *post hoc* interactions,

269   where the control group increased in fractional anisotropy at LD4, but the MMI-treated group did not.

270   This increase in fractional anisotropy was mainly linked to a decrease in radial diffusivity at LD4. At

271   LD4 there was a significant difference between both groups in fractional anisotropy and radial

272   diffusivity. This indicates that the increase in fractional anisotropy at LD4 in the control group was

273   most probably due to increased myelination of these tracts, something that is missing in the MMI-

274   treated group.

275   In conclusion, MMI-induced hypothyroidism did not prevent the overall neuroplasticity to occur

276   during the photosensitive period. Only during the photostimulated phase myelination of several tracts

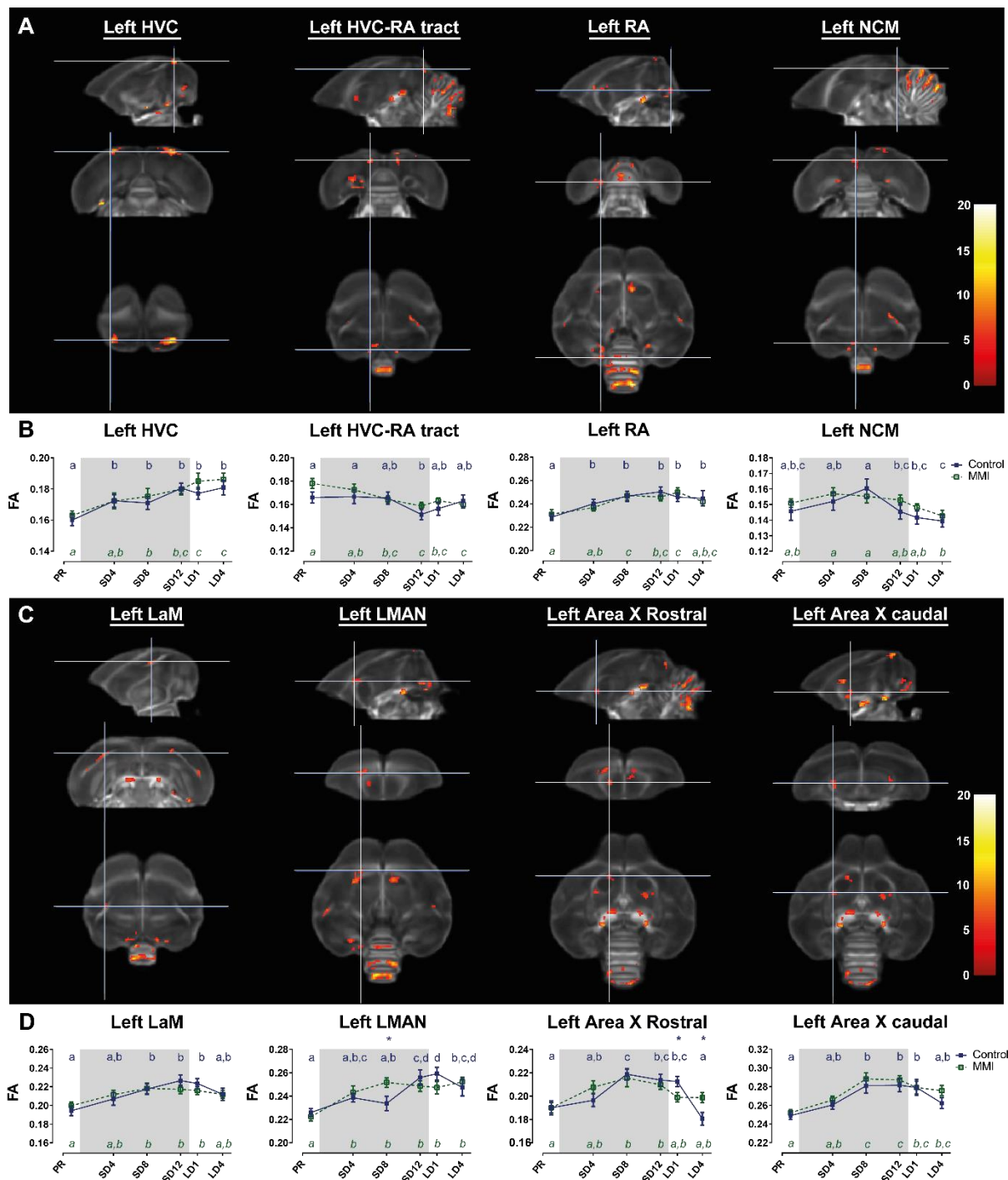277   was affected in the MMI-treated group.

Figure 6: Voxel-based flexible factorial analysis revealed time effect in the song motor pathway and auditory pathway (A), and anterior forebrain pathway (C). The longitudinal changes over time of the extracted diffusion parameter fractional anisotropy of each ROI-based cluster is displayed below (B, D). The statistical maps were assessed at $p_{uncorr}<0.001$ and $k_E≥20$ voxels with a small volume correction including regions of the song control system, white matter structures and the cerebellum. The grey area indicates the photosensitive period of short days (8L:16D). *Post hoc* statistical testing with Tukey's HSD multiple comparison (p < 0.05) correction revealed significant differences between different time points, visualized by different letters. If two time points share the same letter, the DTI values are not significantly different from each other. Significant group differences at specific time points are indicated by *(p < 0.05), ** (p < 0.01) or *** (p < 0.001). Error bars shown are the standard error of the mean.
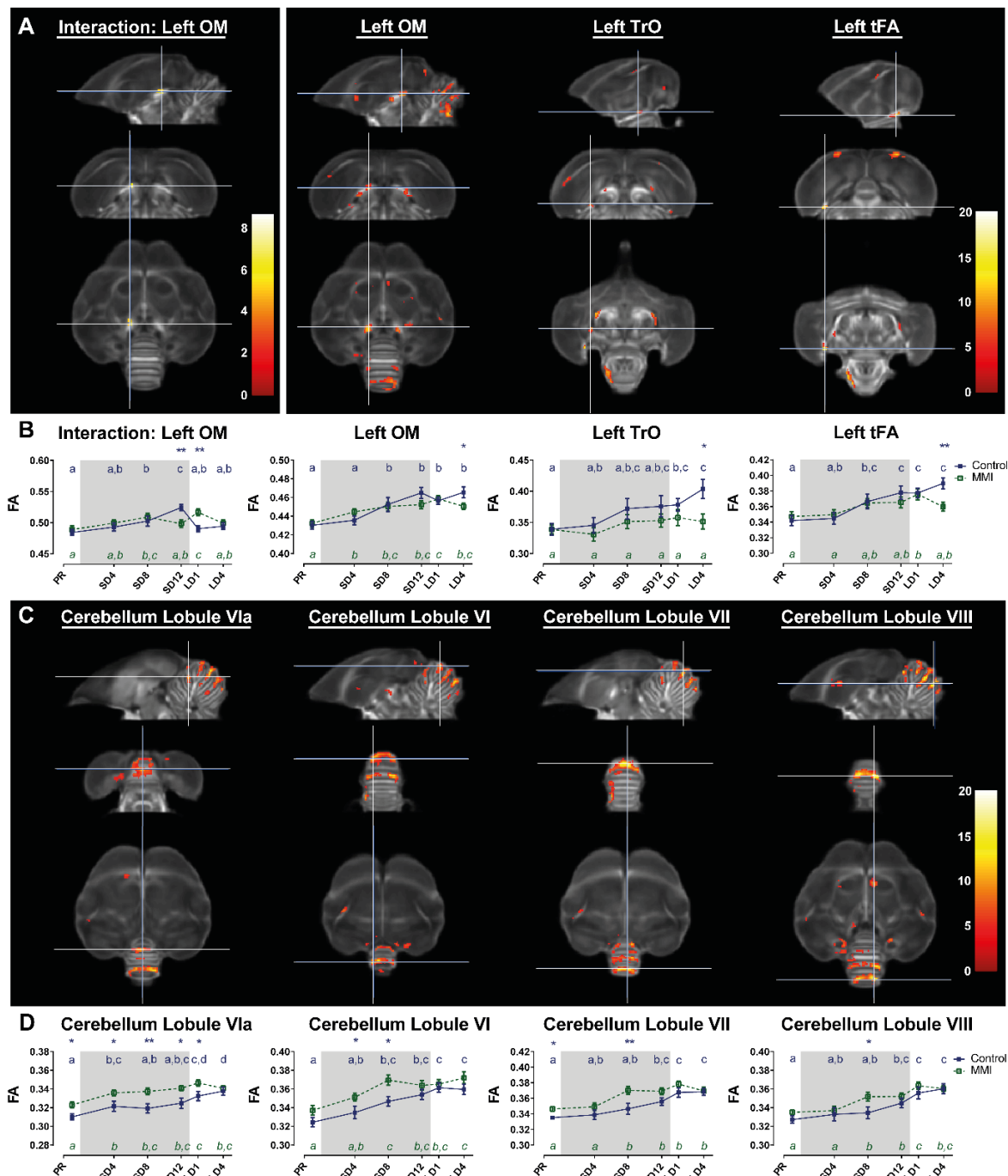
Figure 7: Voxel-based flexible factorial analysis revealed an interaction between time and treatment group in a specific part of the OM tract and time effect in the white matter tracts (A), and specific cerebellar lobules (C). The longitudinal changes over time of the extracted diffusion parameter fractional anisotropy of each ROI-based cluster is displayed below (B, D). The statistical maps were assessed at $p_{uncorr}<0.001$ and $k_E \geq 20$ voxels with a small volume correction including regions of the song control system, white matter structures and the cerebellum. The grey area indicates the photosensitive period of short days (8L:16D). *Post hoc* statistical testing with Tukey's HSD multiple comparison (p < 0.05) correction revealed significant differences between different time points, visualized by different letters. If two time points share the same letter, the DTI values are not significantly different from each other. Significant group differences at specific time points are indicated by *(p < 0.05), ** (p < 0.01) or *** (p < 0.001). Error bars shown are the standard error of the mean.

301 **Table 1: Overview interaction and time effect in fractional anisotropy in small volume correction.**

Effect	Cluster	Hemisphere	Cluster		Peak	
			p_{FWE}	k_E	p_{FWE}	F
Interaction time * group	OM	Left	0.066	25	0.017	8.71
Main time effect	HVC surroundings	Left	<0.0001	80	<0.0001	14.28
		Right	<0.0001	233	<0.0001	16.71
	OM	Left	<0.0001	196	<0.0001	13.45
		Left	0.001	63	0.007	9.18
		Right	<0.0001	124	0.002	9.98
		Right	0.032	30	0.003	9.72
	Area X rostral surroundings	Left	0.007	41	0.266	7.12
		Right	<0.0001	123	<0.0001	10.86
	Area X caudal surroundings	Left	0.002	52	0.054	8.04
		Right	<0.0001	94	0.533	6.55
	tFA	Left	0.001	57	<0.0001	16.39
		Right	0.003	49	0.001	10.14
	Optic tract	Left	0.004	45	<0.0001	17.02
		Left	0.037	29	0.003	9.74
		Right	0.003	48	0.001	10.39
	RA surroundings	Left	<0.0001	96	0.014	8.80
		Left	0.008	40	0.038	8.25
		Left	0.028	31	0.025	8.48
		Right	0.077	24	0.043	8.18
	HVC-RA tract	Left	0.003	49	0.053	8.06
		Right	0.002	52	0.021	8.59
	LMAN	Left	<0.0001	157	0.026	8.45
	Lamina mesopallialis	Left	0.003	49	0.024	8.49
		Left	0.001	57	0.132	7.54
		Right	0.057	26	0.039	8.23
	Caudal NCM	Left	0.011	38	0.225	7.24
	Cerebellum	Lobule VIII	<0.0001	528	<0.0001	20.20
		Lobule VII	<0.0001	741	<0.0001	19.92
		Lobule VIa	<0.0001	271	<0.0001	13.21
		Left side	<0.0001	255	<0.0001	13.15
		Lobule VI	<0.0001	419	<0.0001	12.46

302 Table summarizing the significance at cluster level and peak level. P-values are FWE corrected. K_E indicates the
303 number of voxels within a cluster. Grey values indicate clusters that are significant at cluster level but not at
304 peak level.

305

3.5 Correlations between song behavior, its neural substrate and thyroid hormones

After describing the seasonal neuroplasticity in a general way, we aimed at determining how these neuroplastic fractional anisotropy changes relate to changes in song behavior and hormone levels. Voxel-based multiple regression between song behavior and fractional anisotropy values in the brain was used to determine the location of neural correlates. Interestingly, the song bout length showed a positive correlation to fractional anisotropy values at the level of the left HVC, RA surroundings (bilaterally), left LMAN, left part of the lateral septum (LS) and cerebellar lobules VI-VII whereas a cluster near the HVC-RA tract was negatively correlated to the song bout length (**Figure 8, Table 2**). After extraction of the fractional anisotropy values of the significant clusters, this information was used to determine the within and between-subject correlation of each group separately. This way, we tried to distinguish whether the correlation was present in both groups. Both groups had significant between-subject correlations in all regions, except for the LS that only had a significant between-subject and within-subject correlation in the control group but not in the MMI-treated group (**Table 3**). The correlation to song bout length was largely driven by a between-subject correlation, meaning that birds with longer song bout lengths, had higher fractional anisotropy values in song control nuclei, cerebellar lobules VI-VII and LS. Furthermore, the fractional anisotropy values of the right RA, LMAN and cerebellar lobules VI-VII were also correlated on a within-subject level in both the control and MMI-treated group. Additionally, MMI-treated starlings present a repeated measures correlation at the level of Left RA and right HVC-RA tract, indicating that the variation over time in song bout length was also correlated to the variation in structural neuroplasticity (measured by fractional anisotropy) on a subject level.

Remarkably many of the neuroplasticity changes in the surroundings of the song control nuclei and cerebellum were negatively correlated to the levels of circulating T3 and T4 (**Figure 9, Table 2**). Right HVC, left RA, right Area X surroundings and cerebellar lobules VI-VII were negatively correlated to the circulating T3 levels in both the MMI and control group. As circulating T3 levels decreased during the photosensitive period, whether naturally in the control group or artificially in the MMI-treated group, fractional anisotropy values increased in these regions. This correlation was mostly driven by a between and within-subject correlation in the MMI-treated group (**Table 3**). Only the RA had a significant negative between and within-subject correlation in the control group. Additionally, the control group had significant within-subject correlations to T3 at the level of the right HVC and caudal part of Area X surroundings. Correlations between T4 and the FA values at HVC surroundings and cerebellum only existed in the MMI-treated group. Rather than the natural biological variation in T4

339   in the control group, it is the artificial lowering of the T4 levels by the MMI treatment that correlated
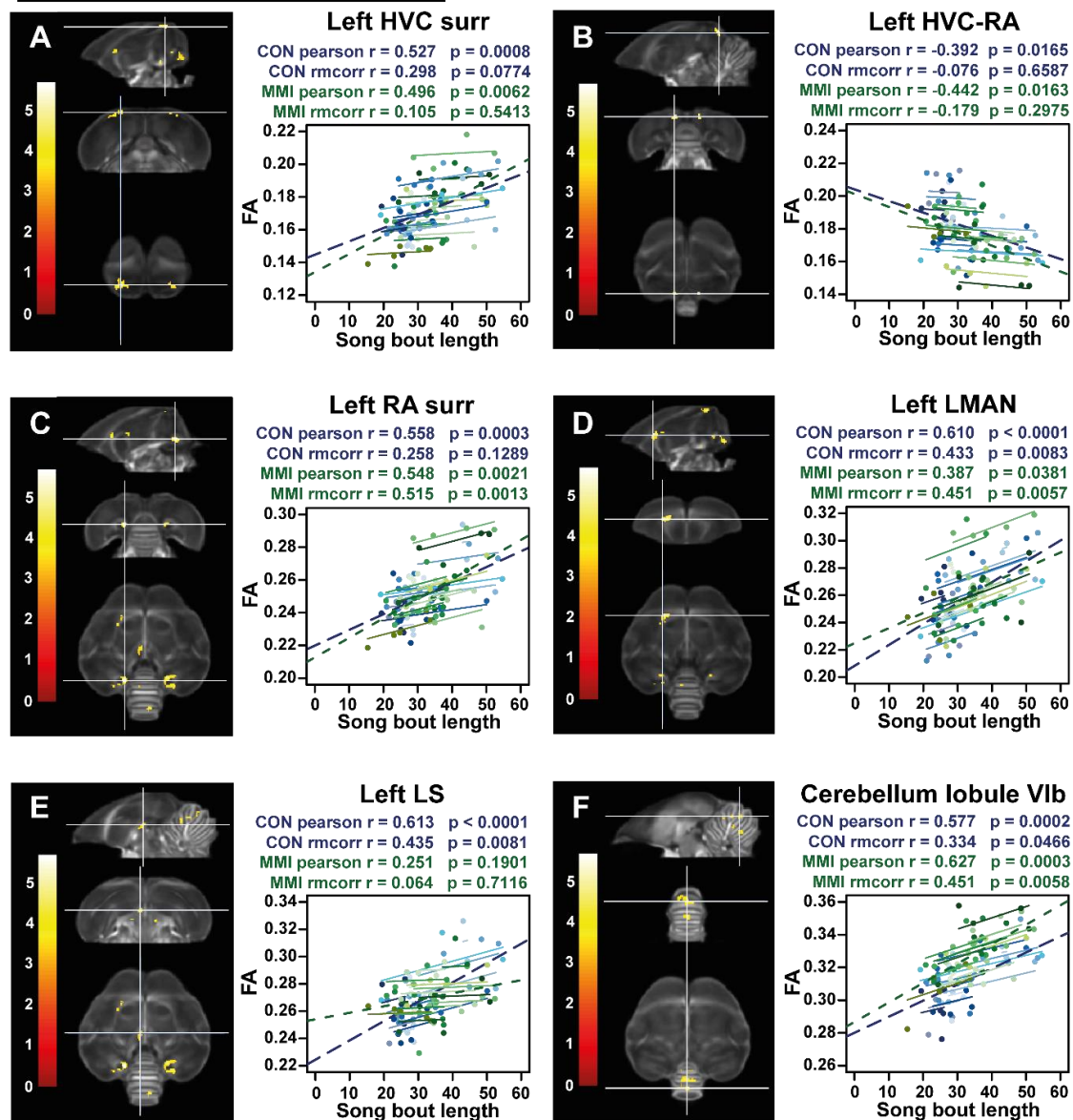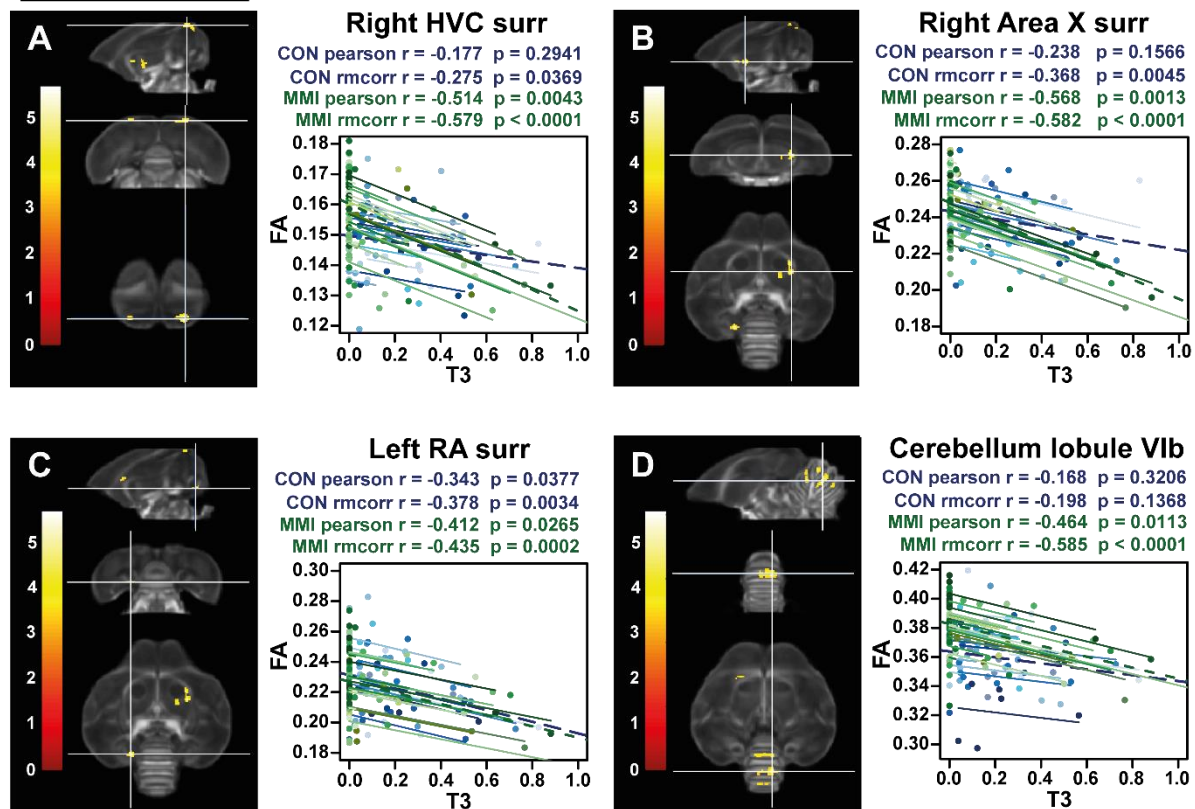
340   to the neuroplasticity in these regions.

Figure 8: Overview of structural neural correlates of song bout length to fractional anisotropy in both groups identified using voxel-based multiple regression. The statistical maps were assessed at $p_{uncorr}<0.001$ and $k_E \geq 20$ voxels with a small volume correction including regions of the song control system, white matter structures and the cerebellum. Below each statistical parametric map, the identified correlations were further explored with repeated measures correlation of the control group (blue) and MMI treatment group (green). Solid colored lines show the best linear fit for the within-subject correlation in the control group (blue) and MMI group (green) using parallel regression lines for individual animals. The blue and green dashed line represent the linear fit of the overall Pearson correlation representing the between-subject correlations of the control and MMI group respectively. For bilateral correlations, only the left side is shown. Abbreviations: surr, surroundings.
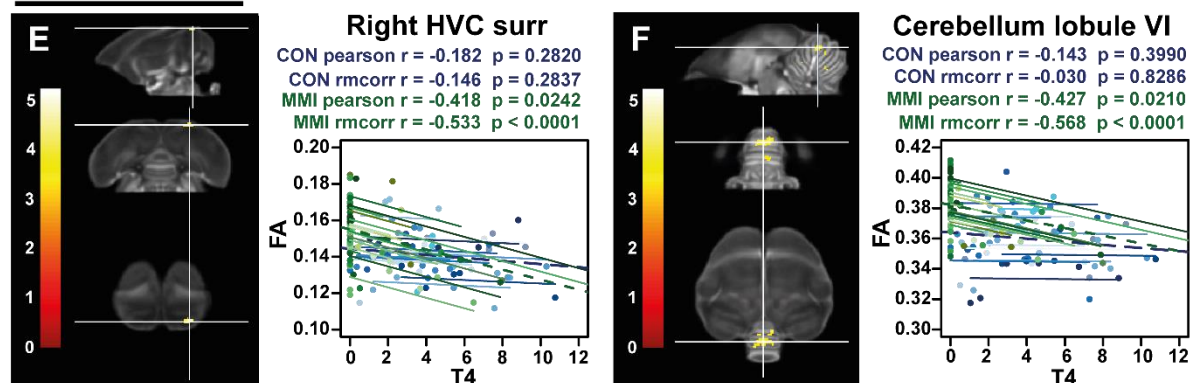
351

Figure 9: Overview of structural neural correlates of thyroid hormones T3 (A-D) and T4 (E-F) levels to fractional anisotropy in both groups identified using voxel-based multiple regression. The statistical maps were assessed at $p_{uncorr}<0.001$ and $k_E≥20$ voxels with a small volume correction including regions of the song control system, white matter structures and the cerebellum. Next to each statistical parametric map, the identified correlations were further explored with repeated measures correlation of the control group (blue) and MMI treatment group (green). Solid colored lines show the best linear fit for the within-subject correlation in the control group (blue) and MMI group (green) using parallel regression lines for individual animals. The blue and green dashed line represent the linear fit of the overall Pearson correlation representing the between-subject correlations of the control and MMI group respectively. For bilateral correlations, only the left side is shown. Abbreviations: surr, surroundings.

362

363 **Table 2: Summary of the voxel-based correlation analysis of song bout length and thyroid hormones T3 and**
364 **T4.**

Effect	Cluster	Hemisphere	Cluster		Peak	
			p_{FWE}	k_E	p_{FWE}	T
Song bout length	RA surr	Left	<0.0001	192	0.005	5.68
		Right	<0.0001	220	0.016	5.39
	HVC surr	Left	<0.0001	136	0.006	5.63
	LMAN	Left	<0.0001	134	0.022	5.31
	Cerebellum	Lobule VIa	0.005	79	0.224	4.58
		Lobule VIb	<0.0001	157	0.069	4.97
		Lobule VII	0.012	65	0.074	4.95
		Lobule VIII	0.045	47	0.190	4,64
	LS	Left	0.033	51	0.472	4.29
	HVC-RA-tract	Left	0.036	50	0.081	4.92
		Right	0.161	31	0.023	5.30
T3	HVC surr	Right	0.005	136	0.003	5.54
	Area X Csurr	Right	0.004	84	0.009	5.28
	RA surr	Left	0.227	28	0.047	4.86
	Cerebellum	Lobule VIb	<0.0001	209	0.008	5.31
		Lobule VI	<0.0001	132	0.011	5.22
		Lobule VIa	<0.0001	171	0.062	4.78
		Lobule VII	0.001	104	0.113	4.62
T4	HVC surr	Right	0.056	46	0.012	5.24
	Cerebellum	Lobule V	<0.0001	214	0.098	4.68

365 This table summarizes for each significant cluster-based ROI the voxel-based FWE corrected p-value at cluster
366 and peak level, next to the overall Pearson's correlation, the repeated measures correlation (rmcorr) and its
367 significance. K_E indicates the cluster size. T reflects the t-value of the maximal peak located within the cluster-
368 based ROI. Voxel-based correlations in grey are significant at the cluster level, but not at peak level.
369 Abbreviations: C, caudal; surr, surroundings.

370 **Table 3: Summary of the overall and repeated measures correlation of song bout length and thyroid hormones**
371 **T3 and T4 for control and MMI-treated group separately.**

	Cluster	Hemi-sphere	Control group				MMI group			
			Pearson		rmcorr		Pearson		Rmcorr	
			r		*r*	*p*	*r*		*r*	*p*
Song bout length	RA surr	Left	**0.558**	**0.0003**	0.258	0.1289	**0.548**	**0.0021**	**0.515**	**0.0013**
	RA surr	Right	**0.575**	**0.0002**	**0.416**	**0.0117**	**0.481**	**0.0082**	**0.371**	**0.0258**
	HVC surr	Left	**0.527**	**0.0008**	0.298	0.0774	**0.496**	**0.0062**	0.105	0.5413
	LMAN	Left	**0.610**	**<0.0001**	**0.433**	**0.0083**	**0.387**	**0.0381**	**0.451**	**0.0057**
	Cerebellum	Lobule VIa	0.366	0.0258	0.385	0.0206	0.596	0.0006	0.490	0.0024
		Lobule VIb	0.577	0.0002	0.334	0.0466	0.627	0.0003	0.451	0.0058
		Lobule VII	0.450	0.0053	0.370	0.0262	0.428	0.0206	0.442	0.0070
		Lobule VIII	0.360	0.0287	0.440	0.0073	0.566	0.0014	0.460	0.0047
	LS	Left	0.613	<0.0001	0.435	0.0081	0.251	0.1901	0.064	0.7116
	HVC-RA-tract	Left	-0.392	0.0165	-0.076	0.6587	-0.442	0.0163	-0.179	0.2975
		Right	**-0.399**	**0.0145**	-0.153	0.4070	**-0.443**	**0.0162**	**-0.380**	**0.0221**
T3	HVC surr	Right	-0.177	0.2941	**-0.275**	**0.0369**	**-0.514**	**0.0043**	**-0.579**	**<0.0001**
	Area X Csurr	Right	-0.238	0.1566	**-0.368**	**0.0045**	**-0.568**	**0.0013**	**-0.582**	**<0.0001**
	RA surr	Left	**-0.343**	**0.0377**	**-0.378**	**0.0034**	**-0.412**	**0.0265**	**-0.435**	**0.0002**
	Cerebellum	Lobule VIb	-0.168	0.3206	-0.198	0.1368	**-0.464**	**0.0113**	**-0.585**	**<0.0001**
		Lobule VI	-0.037	0.8287	-0.026	0.8481	**-0.567**	**0.0013**	**-0.661**	**<0.0001**
		Lobule VIa	-0.150	0.3752	-0.307	0.0192	-0.522	0.0037	-0.610	<0.0001
		Lobule VII	-0.191	0.2564	-0.258	0.0501	-0.378	0.0434	-0.509	<0.0001
T4	HVC surr	Right	-0.182	0.2820	-0.146	0.2837	**-0.418**	**0.0242**	**-0.533**	**<0.0001**
	Cerebellum	Lobule V	-0.143	0.3990	-0.030	0.8286	-0.427	0.021	-0.568	<0.0001

372 This table summarizes for each significant cluster-based ROI the overall Pearson's correlation, the repeated
373 measures correlation (rmcorr) and its significance for control and MMI-treated group separately. Voxel-based
374 correlations in grey are significant at the cluster level, but not at peak level. *Significant correlations are indicated*
375 *in bold.*

376 4.   # Discussion

377   We demonstrate in this study that there are indeed thyroid hormone regulating genes expressed in
378   the song control system, and that expression changes seasonally in the HVC. High *LAT1* expression
379   during the photosensitive phase points to an increased uptake of thyroid hormones in the HVC during
380   this sensitive window of neuroplasticity, whereas during photostimulation, elevated *DIO3* expression
381   limits the amount of active thyroid hormone, presumably to sustain song stability during the breeding
382   season. To establish further the effect of thyroid hormones on song behavior and neuroplasticity, we
383   induced hypothyroidism by MMI treatment. As expected, hypothyroidism inhibited the
384   photostimulation-induced increase in testosterone concentrations in the blood, indicating that as in
385   Japanese quail thyroid hormones play a role in the activation of the HPG-axis upon photostimulation
386   in starlings. The effect of thyroid hormones on testosterone is important for the interpretation of song
387   behavioral changes, since testosterone is known for its effect on song motivation and song quality
388   measures like song bout length (Alward, Balthazart et al. 2013). Somewhat surprisingly,
389   hypothyroidism did not affect the majority of neuroplasticity changes, only the myelination of several
390   tracts during the photostimulated phase were affected. However, it is important to note that even
391   low concentrations of testosterone appear sufficient to induce seasonal neuroplasticity in songbirds
392   (Tramontin, Perfito et al. 2001, Caro, Lambrechts et al. 2005). The presence of a yellow beak in the
393   MMI treated birds meant that there was still some testosterone in the circulation (Ball and Wingfield
394   1987), presumably enough to induce seasonal neuroplasticity. Furthermore, plasma T3 concentrations
395   were negatively correlated to the fractional anisotropy changes in several main song control nuclei,
396   which is in line with the finding that both control and hypothyroid starlings showed decreased thyroid
397   hormone levels during the photosensitive period. We hypothesize that a global reduction of circulating
398   thyroid hormones might be necessary to lift the brake imposed by the photorefractory period,
399   whereas local fine-tuning of thyroid hormone and testosterone concentration through an
400   upregulation of thyroid hormone transporters LAT1 and aromatase activity respectively could activate
401   certain genes and mechanisms associated with neuroplasticity. However the effects of thyroid
402   hormones are complicated by their effect on the HPG-axis and the difference between circulating and
403   intracellular thyroid hormone levels. Therefore, this study is just one of the first steps to disentangle
404   the influence of thyroid hormones on seasonal neuroplasticity and provides a framework for future
405   studies to further investigate the molecular changes induced by thyroid hormones in a seasonal
406   songbird.

4.1 Expression of thyroid hormone inactivating enzyme *DIO3* and thyroid hormone transporter *LAT1* in HVC change over photoperiods.

We established the seasonal expression of several thyroid hormone regulating genes in the song control system using ISH, which is represented in a schematic overview in **Figure 10**. Especially the HVC experiences seasonal differences in thyroid hormone regulating gene expression, namely for *DIO3* and *LAT1*. We validated that our cell counting method was accurate (correlation between cell count and stained surface was > 0.9 for both *DIO3* and *LAT1*) and that these expression levels where not caused by changes in cell density (via Nissl staining **Figure 3 – figure supplement 1**). During the photosensitive phase circulating thyroid hormones are low, but a local upregulation of thyroid hormone transporter *LAT1*, and downregulation of *DIO3* at the level of the HVC, suggests that the local thyroid hormone concentration in the HVC is higher during the photosensitive phase. The downregulation of *DIO3* is not matched by an upregulation of *DIO2*, since there is an apparent lack of *DIO2* expression in the entire telencephalon. All vertebrates need at least a minimum of brain *DIO2* activity to survive but research in chicken and zebra finches already indicated that *DIO2* expression in the brain decreases with age (Van Herck, Delbaere et al. 2015, Raymaekers, Verbeure et al. 2017). Our data seem to confirm that at least in adult birds, *DIO2* expression is too low to be detected by our ISH staining method. This is in stark contrast with what was found during developmental neuroplasticity in the song control nuclei in zebra finches, where the expression of *DIO2* remained high during the sensitive and sensorimotor learning phases (Raymaekers, Verbeure et al. 2017). Several other studies have further suggested that local presence of DIO2 is essential for critical period learning or that correct local balancing of active THs is essential in plastic brain areas involved with learning (Guadaño-Ferraz, Escámez et al. 1999, Yamaguchi, Aoki et al. 2012). In zebra finches DIO2 was most intensively expressed in endothelial cells of blood vessels. Potentially, angiogenesis and hormone supply via the blood-brain barrier are more important and pronounced during developmental neuroplasticity than for adult seasonal neuroplasticity.

Interestingly, several microarray studies in other seasonal songbirds have shown *DIO2* expression in HVC and RA with seasonal changes in expression. Stevenson, Replogle et al. (2012) found that in starlings the *DIO2* expression in RA was the highest during the photosensitive phase, which is in line with our hypothesis of local upregulation of thyroid hormone regulating genes in the song control system during the non-breeding periods. There are however some species differences as Gambel's

438   white crowned sparrows have upregulated *DIO2* expression during breeding conditions in HVC and RA

439   relative to short day conditions (Thompson, Meitzen et al. 2012).

440   The inverse ratio between thyroid hormone transporter *LAT1* and *DIO3* is seen during the

441   photostimulated phase. Even though circulating T4 levels are elevated during this phase, the influx of

442   thyroid hormones and the potential activity of T3 seems to be repressed in the HVC. Local DIO2 and

443   DIO3 activity can fine-tune intracellular thyroid hormone concentration at least partially independent

444   of the circulating thyroid hormone levels. For example in Japanese quail, reciprocal switching of *DIO2*

445   and *DIO3* expression upon photostimulation can locally increase T3 concentration by a 10-fold, even

446   though plasma concentrations do not change (Yoshimura, Yasuo et al. 2003). Interestingly, this could

447   mean that, whereas increased uptake of thyroid hormones by *LAT1* induces neuroplasticity, *DIO3*

448   activity is a possible factor for stability of neural tissue as would be expected in the photostimulated

449   stage.

450   Apart from DIO3 and LAT1, our study also looked at the expression of thyroid hormone receptors and

451   other thyroid hormone transporters. Surprisingly, other thyroid hormone transporters like *MCT8,*

452   *MCT10* or *OATP1C1,* were not detected by ISH in any photoperiod in the starling's telencephalon, even

453   though MCT8 is the transporter with the highest affinity for thyroid hormones (Bourgeois, Van Herck

454   et al. 2016). Several studies, in mammals as well as birds, have shown that MCT8 is highly expressed

455   in the developing brain and is considered as the most important thyroid hormone transporter during

456   developmental neuroplasticity (Van Herck, Geysens et al. 2013, Raymaekers, Verbeure et al. 2017).

457   However, our data suggest that the situation might be different in adult birds, where *LAT1* seems to

458   be more prominent as a mediator in seasonal neuroplasticity.

459   We found *THRA* expression in large parts of the pallium including HVC, RA and LMAN, whereas the

460   striatum including Area X lacked *THRA* expression, which is in line with the expression pattern of *THRA*

461   in adult zebra finches (Raymaekers, Verbeure et al. 2017). In contrast, *THRB* was not detected in any

462   song control nucleus. These observations align with what has been observed in chickens: *THRA*

463   expression seems to be widespread while *THRB* is more locally expressed and exerts some specific

464   functions for brain development (Forrest, Hallböök et al. 1991, Bradley, Towle et al. 1992, Darras, Van

465   Herck et al. 2011, Van Herck, Geysens et al. 2013). Interestingly the expression pattern of *THRA* and

466   *THRB* does not change seasonally, indicating that while at least *THRA* is necessary for proper genomic

467   thyroid hormone action in the song control system, the level of thyroid hormone receptor expression

468   is not a regulatory factor of song control system plasticity.

469   Together these findings suggest an active role for thyroid hormones during the non-breeding phase
470   to induce plasticity in the song control system, in contrast to the photostimulated phase where thyroid
471   hormones are locally decreased in the HVC to promote stabilization of the song **(Figure 12)**.
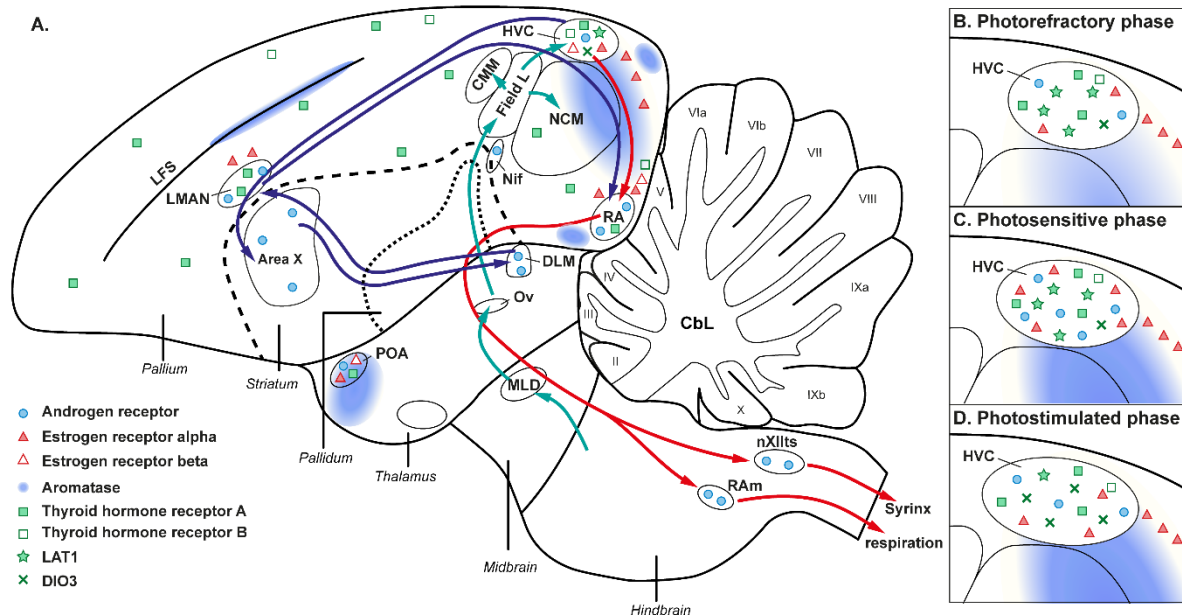

472

Figure 10: Schematic overview of the steroid and thyroid hormone receptors within the songbird brain (A) and how this expression changes seasonally at the level of the HVC (B - D). Androgen receptor, estrogen receptor and aromatase expression is based on prior studies in starlings and canaries (Gahr 1990, Bernard, Bentley et al. 1999, Metzdorf, Gahr et al. 1999). The expression of thyroid hormone regulating genes is derived from our own results. (B-D) In canaries the estrogen and androgen receptor expression is higher during photosensitive and early photostimulated phase compared to the photorefractory state (Gahr and Metzdorf 1997, Fusani, Van't Hof et al. 2000). In starlings aromatase activity and androgen receptor density was the highest during the photosensitive phase (Riters, Baillien et al. 2001) (Riters, Eens et al. 2002).

4.2 Thyroid hormones regulate HPG-axis activity in starlings

482   In the second experiment, we deprived the starlings of circulating thyroid hormones by MMI
483   treatment during the photosensitive and photostimulated phase to investigate their effect on
484   testosterone, song and neuroplasticity. MMI is an anti-thyroid drug inhibiting the synthesis of T3 and
485   T4 at the level of the thyroid gland, thereby gradually depleting circulating thyroid hormone levels.
486   MMI treatment was started on the first short day of the photosensitive period, as earlier treatment
487   could terminate the photorefractory period (Dawson, Goldsmith et al. 1985). After 4 weeks of MMI
488   treatment thyroid hormone levels were successfully depleted, which is consistent with the findings in
489   Japanese quail, where MMI treatment for 4 weeks resulted in decreased thyroid hormone levels,
490   testes weight and testosterone levels (Weng, Saita et al. 2007). In immature rats MMI affected the
491   HPG-axis, decreasing luteinizing hormone (LH) and testosterone plasma concentration, but also
492   decreased the testes binding sites for LH by 30% (Valle, Oliveira-Filho et al. 1985, Pérez, Meddle et al.

2018). The present results show that hypothyroidism also inhibited the photostimulation-induced increase in testosterone in starlings. Yoshimura, Yasuo et al. (2003) demonstrated that in Japanese quail thyroid hormones play a crucial role in the activation of the HPG-axis upon photostimulation. Exposure to long days increases hypothalamic T3 concentration as a result of a local upregulation of *DIO2* and downregulation of *DIO3* in the mediobasal hypothalamus. This locally produced bioactive T3 subsequently results in morphological changes in GnRH nerve terminals enabling GnRH secretion resulting in activation of the HPG-axis (Yoshimura 2013). In starlings under natural photoconditions, this phenomenon was observed to a lesser extent, but it did not corroborate the proposed photoperiodic regulation of the HPG-axis through *DIO2/DIO3* expression (Bentley, Tucker et al. 2013). It is suggested that both phylogenetic differences and the acuteness at which photoperiods are changed in experiments might influence the changes in hypothalamic thyroid hormone regulation. Likely, the regulatory mechanisms in natural conditions are similar but more gradual. In agreement with manipulation studies in quail where the DIO2 inhibitor iopanoic acid prevents testicular growth (Yoshimura, Yasuo et al. 2003), our manipulation study confirms the active role of thyroid hormones in the activation of the HPG-axis **(Figure 12)**.

4.3 **Hypothyroidism affects song behavior by depleting testosterone**

Of particular interest is the relationship between hormonal changes, song behavior and neuroplasticity as they change over the different seasonal states that were induced by the photoperiodic manipulations (schematic overview in **Figure 11**). By using *in vivo* techniques such as MRI, we established that song bout length is positively correlated to the testosterone levels, beak color and neuroplasticity associated fractional anisotropy changes (**Figure 11**). The correlation between song bout length and testosterone is only present in the control group, since MMI treatment inhibited the photostimulation-induced increase in testosterone. However, beak color was still correlated to the song bout length in the MMI group, indicating that even low concentrations of testosterone, below detection limit of the RIA assay but enough to induce beak color changes, are linked to changes in song bout length. The neural substrate of song bout length includes, as expected, song control nuclei like HVC, RA and LMAN, which concurs with earlier correlation studies in starlings and other songbirds (Bernard, Eens et al. 1996, Garamszegi and Eens 2004). However, also other structures like the lateral septum and cerebellar lobule VI-VII are correlated to song bout length. At the level of the lateral septum Merullo, Cordes et al. (2015) showed a positive correlation between neurotensin (a neuropeptide that regulates dopamine activity) expression and both sexually motivated song and non-vocal courtship behaviors in starlings. Whereas in songbirds, only few studies looked at the role of the cerebellum in song behavior through the cerebello-thalamic-basal ganglia

526   pathway (Person, Gale et al. 2008, Nicholson, Roberts et al. 2018, Pidoux, Le Blanc et al. 2018), in

527   humans, the cerebellum is known to be involved in language tasks (lobule VI and crus I/II) and

528   phonological storage during the maintenance of verbal information (VIIb/VIII). Prior lesion study

529   showed that lesioning Area X caused structural remodeling of the cerebello-thalamic-basal ganglia

530   pathway extending into cerebellar lobules VIb and VII (Hamaide, Lukacova et al. 2020). Our results

531   further corroborate that cerebellar lobules VI-VII retain the neural substrate for song behavior.

532   Furthermore, these parts of the cerebellum show seasonal neuroplasticity, both in male and female

533   starlings (Orije, Cardon et al. 2021).

534   The absence of high testosterone levels in hypothyroid starlings during the photostimulated phase

535   could explain some of the differences in song behavior. Even though song rate did not change

536   significantly over time in both groups, hypothyroid starlings sang with a lower song rate during

537   photostimulation compared to the control group. Testosterone is known to increase the motivation

538   to sing, by interacting with the medial pre-optic nucleus (POM), since local testosterone implantation

539   in the POM of castrated male canaries increased their song rate (Alward, Balthazart et al. 2013).

540   Interestingly, hypothyroid starlings keep on increasing their song bout length during the

541   photostimulated phase, compared to the control group, which sing at a stable song bout length during

542   photostimulation. This lack of stability in the song bout length during photostimulation could be due

543   to the absence of high testosterone concentrations, as testosterone is known to be necessary for song

544   crystallization and stabilization in sparrows, zebra finches and canaries (Marler, Peters et al. 1988,

545   Korsia and Bottjer 1991, Williams, Connor et al. 2003). Blocking testosterone by castration or by the

546   androgen receptor antagonist flutamide, causes variability in song of zebra finches and canaries

547   (Wang, Liao et al. 2014, Alward, Balthazart et al. 2017). More specifically blocking androgen receptors

548   in the RA of male canaries, caused song duration to increase, whereas specific blocking in HVC

549   increased the variability in used syllables (Alward, Balthazart et al. 2017) **(Figure 12)**.

550   Many early studies concluded that relatively high testosterone concentrations seem to be involved in

551   high song rate and song stability during the photostimulated phase or the annual cycle. More recent

552   studies have found that low concentrations of testosterone are sufficient to induce seasonal

553   neuroplasticity (Tramontin, Perfito et al. 2001, Caro, Lambrechts et al. 2005). In our study, changes in

554   beak color represented low concentrations of testosterone that are biologically active and correlated

555   to song bout length, which has its neural substrate in several song control nuclei, lateral septum and
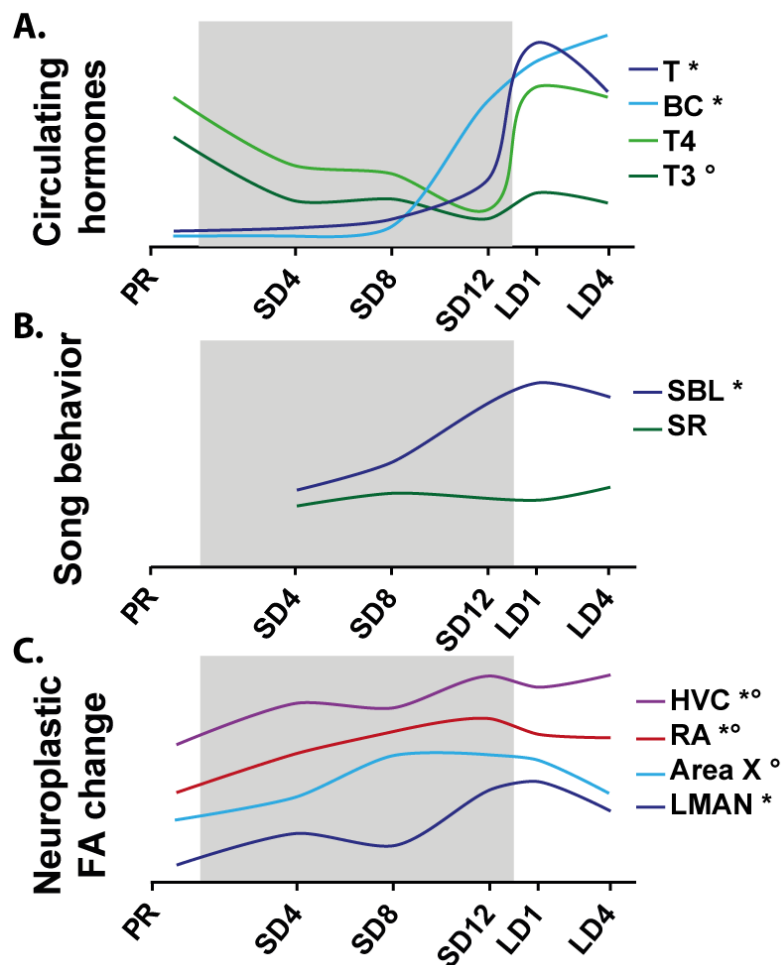
556   cerebellum.

557

Figure 11: Schematic overview of the seasonal changes in circulating hormones, thyroid hormone (TH) and testosterone (T), song behavior and neuroplasticity changes in fractional anisotropy (FA). Correlations to song bout length (SBL) and T3 are indicate by * and ° respectively. The grey area indicates the photosensitive period. Abbreviations: BC, beak color.

4.4 Complex interaction between thyroid hormones and neuroplasticity

Deprivation of thyroid hormones during the photosensitive period did not prevent neuroplasticity from occurring. In contrast, certain regions within the MMI group showed earlier significant differences in FA during the short days compared to the control group, pointing to an earlier onset of neuroplasticity coinciding with the earlier depletion of T3 and T4. Under natural conditions, the level of circulating thyroid levels is low during the photosensitive period. By administrating MMI, we rapidly decrease circulating thyroid hormone levels to a minimum. The decrease of circulating thyroid hormones is necessary to terminate the photorefractory period for the reproductive system (Dawson, Goldsmith et al. 1986). The photorefractory period depends on thyroid hormones to prevent reproductive maturation in response to long day length (Nicholls, Goldsmith et al. 1988).

573   Photorefractoriness not only forms a brake on gonadal maturation but also prevents an increase in

574   singing activity in response to testosterone treatment, in contrast to photosensitive female starlings

575   treated with testosterone (Rouse, Stevenson et al. 2015). Potentially, the global reduction of

576   circulating thyroid hormones is necessary to lift the brake on singing and on reproduction imposed by

577   the photorefractory period. Interestingly, the circulating T3 level presents a negative within-subject

578   correlation to neuroplasticity in HVC, Area X and RA surroundings both in the control and hypothyroid

579   group, indicating that decreasing circulating thyroid hormone levels are associated with the

580   neuroplasticity during the photosensitive phase. This negative correlation between T3 and

581   neuroplasticity seems in contrast to the thyroid hormone regulating genes in HVC, which supports an

582   active role of thyroid hormones during the photosensitive phase. We hypothesize that while a global

583   reduction in thyroid hormones is necessary to lift the brake imposed by the photorefractory period,

584   local fine-tuning of thyroid hormone concentration through thyroid hormone regulating proteins like

585   LAT1 and DIO3 could activate mechanisms associated with neuroplasticity. A similar local fine-tuning

586   of testosterone levels during the photosensitive phase has been suggested by Riters, Baillien et al.

587   (2001). They found increased aromatase activity and decreased 5β-reductase activity during the

588   photosensitive period in male starlings, increasing the brain's sensitivity to testosterone despite the

589   low circulating testosterone levels (**Figure 10**).

590   Prior studies have shown that the photosensitive phase acts as a sensitive window for multisensory

591   neuroplasticity (Cornez, Collignon et al. 2020, Orije, Cardon et al. 2021). Multiple studies looked at

592   potential causes for the reopening of a critical or sensitive period and there seem to be two main

593   components involved: (1) the balance between the excitatory-inhibitory (E-I) circuits and (2) the

594   molecular brakes that are imposed to limit adult neuroplasticity. After an initial critical period,

595   neuroplasticity can be reintroduced when the E-I balance shifts more towards the excitation rather

596   than inhibition due to increased excitation or reduced inhibition. Whether and how thyroid hormones

597   directly partake in the regulation of molecular mechanisms of reopening a sensitive window in vocal

598   learning remains to be elucidated. Thyroid hormone function is complex, some genes are upregulated

599   in the presence of T3 (positively regulated genes), whereas some genes are down-regulated

600   (negatively regulated genes). Gil-Ibanez, Garcia-Garcia et al. (2017) showed that both positively and

601   negatively regulated genes can play a role in neuroplasticity. Further studies are required to identify

602   the genetic expression changes upon thyroid hormone manipulation in starling brain, and to establish

603   how these genetic changes affect neuroplasticity.

604   At the end of the photosensitive phase, the sensitive window closes by imposing molecular brakes like

605   PNN and myelin. PNNs are highly expressed in the HVC of adult zebra finches after their song learning

606   and predicts song maturity (Balmer, Carels et al. 2009). However, starlings have far less PNNs,

607   compared to closed-ended learning zebra finches, suggesting that PNN might play less of a role in the

608   control of seasonal neuroplasticity of open-ended learning starlings (Cornez, Madison et al. 2017). Our

609   prior studies suggested myelination rather than PNNs as another candidate mechanism that

610   contributes to ending a sensitive window in open-ended learners like starlings (Orije, Cardon et al.

611   2021). In the control group, several tracts including OM, TrO and tFA increased in fractional anisotropy

612   upon photostimulation, due to decreased radial diffusivity, which implies an increase in myelination.

613   This increased fractional anisotropy was absent in the MMI-treated group, which could reflect the

614   thyroid hormone effect on myelination. Myelin basic protein is a positively regulated thyroid hormone

615   dependent gene, which could respond to the normally increased T4 plasma concentrations during the

616   photostimulated phase. Furthermore, thyroid hormone therapy was shown to induce myelinogenesis

617   in an animal model of demyelination (Harsan, Steibel et al. 2008). So increased levels of testosterone

618   and thyroid hormone levels during photostimulation could play a role in ending a sensitive window

619   for plasticity in song behavior and its underlying neural structure through myelination acting as a
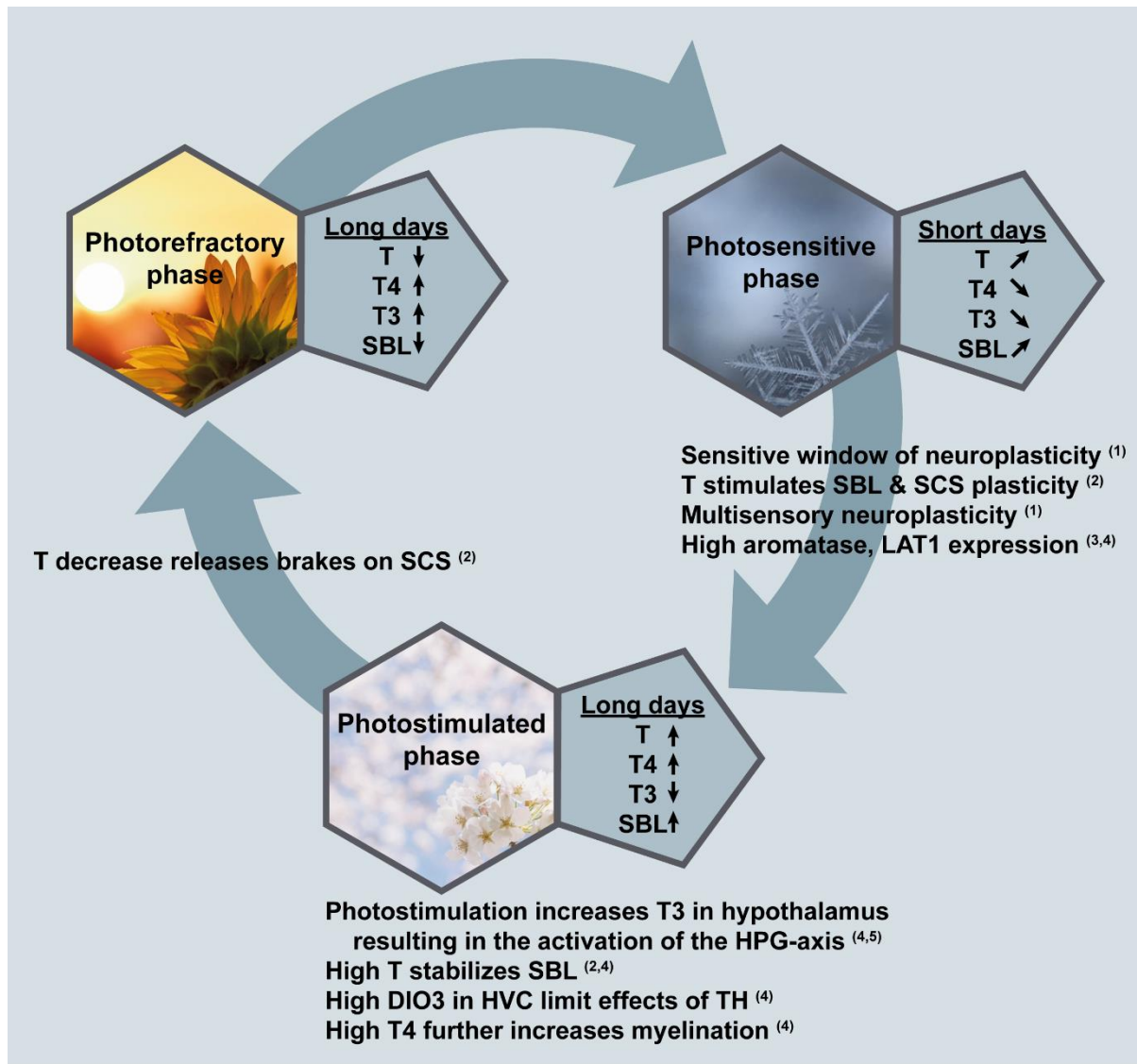
620   molecular brake **(Figure 12)**.

Figure 12: Schematic overview summarizing the seasonal changes in hormones, song behavior and neuroplasticity found in the current study and the hypotheses derived from this and prior studies. For each seasonal stage the plasma hormone concentrations (testosterone (T), thyroid hormones (TH) thyroxine (T4) and triiodothyronine (T3)) and song bout length (SBL) as a read out for song quality were summarized. During the short days of the photosensitive period, plasma T concentrations and SBL gradually increase, while plasma T4 and T3 concentrations gradually decrease. This period was demonstrated to be a sensitive window for increased neuroplasticity in the song control system (SCS), all sensory systems and the cerebellum (see (1) (Orije, Cardon et al. 2021)). During this period, T can induce increased SBL and SCS neuroplasticity (see (2) Orije, Cardon et al. (2020)). Even though the circulating concentrations of T and thyroid hormones are low, their effects might be maximized by local fine-tuning through upregulation of aromatase in the telencephalon (see (3) Riters, Baillien et al. (2001)) and thyroid hormone transporter LAT1 in HVC (see **Figure 2** of this study (4)). Upon long days during photostimulation, T3 levels increase in the hypothalamus resulting in the activation of the HPG-axis (see (5) Yoshimura (2013)). The resulting peak in T levels coincided with high SBL and T4 levels. These high T levels help to stabilize the SBL during this phase. High DIO3 expression in the HVC represses the potential activity of T3 or T4, preventing further neuroplasticity in order to promote song stability (see **Figure 2** of this study (4)). In other parts of the brain, high T4 is required for myelination and hence consolidation of several white matter tracts that were modulated and shaped in the photosensitive stage (see **Figure 7** of this study (4)). Continuation of long days eventually leads to the photorefractory phase, where T levels decrease again due to gonadal regression, thereby releasing again the brakes of neuroplasticity on the SCS and allowing the song to become plastic again (see (2) Orije, Cardon et al. (2020)).

4.5 **Future perspectives**

Methimazole treatment did not only drastically reduce thyroid hormones to a minimum, it also inhibited the increase of testosterone upon photostimulation. In the current study we altered both thyroid and testosterone concentrations. Future studies might want to control the amount of circulating testosterone by castration or testosterone implantation during photostimulation, to be able to solely investigate the effects of thyroid hormone manipulation. This way the suggested effect of thyroid hormone on myelination of several tracts during the photostimulated phase could be attributed to the lack of thyroid hormone's positive effect on myelination, if myelination is still affected with MMI treatment combined with testosterone supplementation during photostimulation.

Importantly, methimazole treatment does not completely abolish thyroidal hormone production and thus low concentrations of thyroid hormones could still be locally picked up within the brain, as suggested by the increased LAT1 expression in the HVC. Future studies could consider other manipulations to investigate the effects of thyroid hormones on neuroplasticity in songbirds and their song behavior. For example, iopanoic acid both inhibits thyroid hormone release from the thyroid gland but also the conversion of T4 to T3 by inhibiting DIO2, but it is less practical for long term treatment strategies (Pant and Chandola-Saklani 1993). In the past both surgical and radioactive thyroidectomy have been applied to study the effects of thyroid hormones on seasonal reproduction (Dawson, Goldsmith et al. 1986, Bentley, Dawson et al. 2000). Analogous to experiments examining the local effects of testosterone by local androgen receptor inhibition (Alward, Balthazart et al. 2017), thyroid hormone antagonists and thyroid hormone receptor modulators have been developed and could be injected locally within specific song nuclei, to investigate their role in song behavior (Lim, Nguyen et al. 2002, Yoshihara and Scanlan 2003, Raparti, Jain et al. 2013).

664 ## 5. Material & Methods

665 ### 5.1 **Subjects & Experimental setup**

666 Wild European starlings (Sturnus vulgaris) used in the *in situ* hybridization experiment were caught in
667 Baltimore, USA during mid-late winter 2013 and subsequently treated by the research group of prof.
668 Gregory Ball. 24 male adult starlings were divided in 3 groups of 8, and treated in order to represent
669 the photosensitive, photostimulated and photorefractory states. All birds were initially maintained on
670 short day lengths (8 hours of light, 16 hours of dark, 8L:16D) to keep them in a photosensitive state.
671 Photoperiod manipulations were applied over a period of 12 weeks. Group 1 was immediately put on
672 long day lengths (14L:10D) for 12 weeks so they would be photorefractory by the end of photoperiod
673 manipulation. Group 2 was kept on 8L:16D for 12 weeks so that they would remain photosensitive.
674 Group 3 was kept on 8L:16D for 8 weeks, then switched to long day lengths (14L:10D) for 4 weeks to
675 make them photostimulated. In order to control for handling stress associated with transferring group
676 2 to a different photoperiod, all groups were transferred into a new cage located within the same
677 room. Birds remained with the same cage mates throughout the entire experiment. No females were
678 present in any group. While studies showed that the presence of females influences neurological
679 attributes and singing rate in canaries (Alward, Mayes et al. 2014, Shevchouk, Ball et al. 2017), and
680 even slightly increases the growth of the sparrow HVC and RA compared to isolated birds, photoperiod
681 is still the main instigator of song control nucleus growth (Tramontin, Wingfield et al. 1999).

682 Food and water was supplied *ad libitum*, and supplementary spinach was provided daily. In order to
683 verify sex and measure testis growth, exploratory laparotomies were performed prior to placing birds
684 into their experimental groups. Under isoflurane anesthesia, a small incision was made on the bird's
685 left side, and calipers were used to measure the testis diameter. The incision was closed with nylon
686 sutures, and birds were allowed to recover for one week. After one week, they were placed into the
687 appropriate experimental groups. At the end of the 12 week period, all birds were anesthetized via
688 injection of secobarbital followed by cardiac perfusion with 4% paraformaldehyde. Brains were
689 dissected out and placed into 4% paraformaldehyde. The testes were dissected out, measured with
690 calipers and weighed. Bird body weights were recorded, and the color of their beaks was scored to
691 monitor physiological response to the photoperiod. All procedures were in accordance with the animal
692 welfare regulations of the John Hopkins University of Baltimore, Maryland, USA. Brains were quickly
693 frozen, stored at -80 °C and sent to the research group of Comparative Endocrinology at the KU Leuven
694 together with blood samples, where all subsequent procedures took place.

695   The second experiment was performed on thirty male starlings (*Sturnus vulgaris*) that were wild
696   caught as adults in Normandy (France) in November 2014. All animals were housed in two large indoor
697   aviaries (L x W x H: 2.2 x 1.4 x 2.1 m) at the University of Antwerp with food and water ad libitum with
698   artificial light dark cycle. Starting from January 2013, all birds were kept in a long day photoperiod
699   (16L/8D) in order to remain photorefractory. The housing and experimental procedures were
700   performed in agreement with the Belgian and Flemish laws and were approved by the Committee on
701   Animal Care and Use of the University of Antwerp, Belgium (2014-52).

702   Starlings were divided into two groups: a hypothyroid group (N=16) and a control group (N=14). The
703   study was started when all birds were photorefractory. Then they were switched from long to short
704   (8L:16D) days to induce the return to photosensitivity. Methimazole (MMI) treatment was started in
705   one group to induce hypothyroidism. By supplementing the drinking water with 0.05% MMI, the
706   endogenous stock of THs gradually decreased until it was fully depleted after 2-3 weeks. MMI
707   treatment was continued for the remainder of the experiment. After 12 weeks of short days, the
708   photosensitive starlings were switched back to long days (16L:8D) so that they became
709   photostimulated. In parallel the control group was exposed to the same photoperiodic regime without
710   receiving any hormone manipulation.

711   We monitored the neuroplasticity repeatedly at 6 different time points. The first time point was at the
712   end of the photorefractory state (PR). After switching to short days we measured every 4 weeks to
713   follow up the song control system plasticity during the photosensitive period (SD4, SD8, SD12).
714   Additionally, we measured after 1 week of long days, as it is known that exposure to 1 long day can
715   already affect TH.

716   Finally, we measured after 4 weeks on long days (LD4), when starlings were fully photostimulated. At
717   each time point, songs were recorded, blood samples were taken, and MRI (DTI and 3D) was acquired.
718   In addition body weight and beak color were registered.

5.2 *In situ* hybridization

720   30 μm thick coronal brain sections were made using a cryostat and kept free floating in cryobuffer
721   (1.59 g/l NaH2PO4, 5.47 g/l Na2HPO4, 300 g/l sucrose, 10 g/l polyvinylpyrrolidone and 300 ml/l
722   ethylene glycol in RNase free H2O) in 24 series so that each subsequent section in a series was 720
723   μm apart from the previous one. Sections were stored in cryobuffer at -20°C until used.

5.2.1 DNA cloning and probe synthesis

DNA cloning and probe synthesis of a partial sequence of the target genes in starling was done similarly to the method used for zebra finch genes (Raymaekers, Verbeure et al. 2017). RNA was isolated from the brain of an adult male starling. The primers used for cloning are shown in **Table 4**. Cloning was successful except for the sequence of OATP1C1. Therefore, we instead used the corresponding probe for zebra finch (Raymaekers, Verbeure et al. 2017) that has 94% sequence homology with the corresponding starling sequence, which is sufficient to generate specific signal.

Table 4: Primers for cloning of partial sequences of thyroid hormone regulators in starling.

Gene	Forward primer (5'-3')	Reverse primer (5'-3')	NCBI Accession no.
DIO2	ATAGCCAAGGGCAGTGATGG	CACCCTACCTGCTTGACAGC	XM_014869830
DIO3	GTGTCCGACTCCAACTGCAT	TGGTCTAGCCAGCTCCTCAG	XM_014871958
MCT8	ATCGTCAGCATCTTCACCGA	ATGGTGGTGAAGAAGCCATC	XM_014877151
MCT10	AGACCTGTTTGGCTGTCGAA	GACAGCAACGAGAGCTCCAA	XM_014879264
OATP1C1	CAAACAGCACAGTCTTGCCC	CAGCTATCAGGTAGCCCAGC	XM_002196271.2
LAT1	CGCCTACATGCTGGAGGTTT	AGAACAGCCGGGAAGAAGTG	XM_014874486
THRA	AGATGAACAGTGTGTGGTGT	ACTTGCCGAGGTCGAAGATG	XM_014885513
THRB	TGCCAGGAATGTCGCTTCAA	AGTGTTCGAATGCCAGGAGG	XM_014887263

5.2.2 *In situ* hybridization staining

The ISH protocol used for detection of thyroid hormone regulator genes in starling closely resembled the protocol used for zebra finch (Raymaekers, Verbeure et al. 2017). From each series, sections containing song control nuclei were selected and placed individually in wells of a 24-well plate. This was on average 3 sections for Area X, 2 for LMAN, 2 for HVC and 2 for RA. Of each photoperiod, one brain was omitted from staining due to cutting or freezing damage; thus the number of birds (N) stained for each photoperiod was 7. ISH was performed with both anti-sense and sense (negative control) probes.

5.2.3 Nissl staining

Of 3 birds of each photoperiod, 2 HVC sections, 720 µm apart, were stained with cresyl violet. Sections were rinsed in PBS, incubated in 1% cresyl violet in H_2O for 1 min and then rinsed three times in H_2O containing 2.5% acetic acid for 1 min. Sections were again rinsed in H_2O, mounted onto glass slides, incubated in xylene for 30 seconds and coverslipped with DPX (Sigma).

5.2.4 *In situ* hybridization imaging and data analysis

Photomicrographs in the regions of interest were taken for all markers using a stereomicroscope (Carl Zeiss). Data in HVC from the *DIO3* and *LAT1* ISH and the Nissl staining were quantified (on average 2 sections per bird for each marker) using Fiji software (ImageJ, National Institute of Health) and statistically analyzed using GraphPad Prism 5 (GraphPad Software, Inc.). We only analyzed 1 side of each section, selecting a 100 000 μm² square box was selected in the middle of HVC (central on the mediolateral and dorsoventral axes through the nucleus). Inside that box, *DIO3+* cells, *LAT1+* cells and cells stained by cresyl violet were counted. Cells were counted as a 'stained cell' if the dark signal was delineated in the form of at least a semicircle (180 degrees or more) around the center. Cell counts of both sections from one bird were then averaged to obtain 1 numerical value per bird. Signal throughout HVC was generally homogeneously spread, but for rare sections with heterogeneous signal, larger areas were analyzed and data normalized. We analyzed the differences in *DIO3+, LAT1+* or Nissl stained cells between photoperiods using a linear mixed model. When appropriate, further comparisons were performed with the Bonferroni *post hoc* test or Dunn's *post hoc* test respectively to analyze differences between two photoperiods.

To further evaluate the validity of the cell count method used for the *DIO3* and *LAT1* ISH, 10 random sections of both ISHs were analyzed using the semi-quantitative manner of 'stained surface fraction' as used for the zebra finches (Raymaekers, Verbeure et al. 2017). For each section, a 100 000 μm² square box was selected in the middle of HVC (central on the mediolateral and dorsoventral axes through the nucleus). The image was converted to greyscale (each pixel is assigned a brightness value between 0 and 255) and a brightness threshold was manually set for each image so that dark staining was counted as 'stained' while background was not. This way, the stained surface area was calculated and divided by the total area of the 100 000 μm² box. The stained surface fraction values were plotted against their corresponding original cell count value. Linear regression analysis was performed and the coefficient of determination (r^2) was calculated using Prism 5 to check for correlation.

5.3 **Blood sample analysis**

At each time point of the hypothyroidism experiment blood samples were taken to assay plasma levels of T3, T4 and testosterone. In order to limit variation of plasma levels due to the time of the day, blood samples were taken at each stage within a 2 hour window at noon between 11u30 and 13u30. Animals were already subdivided in small cages for individual song recordings. This allowed fast capture and blood sampling (within 5 min.) to minimize increase in testosterone as a result of acute stress (Van Hout, Eens et al. 2010). The alar wing vein was punctured with a 25-gauge needle to collect 300-500

777 µl of blood into heparin-coated capillary tubes. Blood samples were centrifuged for 10 min at 2060g

778 while cooling to 4°C. After centrifugation, the plasma was collected and frozen at -20°C, where the

779 samples remained until analysis. Radioimmunoassay for testosterone, T3 and T4 were performed as

780 described previously in (Orije, Cardon et al. 2021) and (Reyns, Janssens et al. 2002) respectively.

781 ## 5.4 **Song analysis**

782 Song was recorded with Behringer C-2 condensator microphones, connected to a PR8E multi-channel

783 preamplifier (SM Pro audio) and 'Delta Series' Breakout box (M-audio). The microphones were placed

784 on top of individual cages. Due to technical issues, songs of birds were lost at PR and SD12 in both

785 groups and at SD4 in the MMI treated group. Since fully isolated starlings do not sing as they would

786 do in group context, the individual cages were placed next to the aviary. Using SoundExplorer

787 (Developed by RF Jansen, University of Amsterdam) sonograms were created of the recordings. Based

788 on the intensity and the spectral definition of the song bouts, individual song could be differentiated

789 from background noise of the aviary. In line with prior song processing (Eens 1997, Van Hout, Pinxten

790 et al. 2012) we defined a song bout as a period of at least 5s of song with pauses no longer than 1.5s.

791 Starling song consists out of 4 distinct phrases, which are mostly performed in a fixed order. The song

792 often starts with one or several whistles (whistle phrase), followed by a section of complex phrases

793 (variable phrases) and rapid series of clicks or rattles (rattle or click phrase), before ending the song

794 with high frequency song elements (high frequency phrases). Song bouts containing at least three

795 different phrases were labelled as 'complete song bouts'. Analysis of the song bout length was only

796 performed on complete songs. If there were no complete song bouts at a certain time point, the

797 average song bout length of incomplete songs was calculated and taken as a measure of the evolution

798 in song production.

799 At each photoperiod songs were recorded for 48 hours. The song bout length measured in seconds

800 and singing rate (average minutes spent singing per hour) were quantified as a measure of the singing

801 behavior. The song rate was calculated as the average number of complete song bouts per hour.

802 Statistical analysis of testosterone levels and song behavior was performed using linear mixed model

803 via JMP Pro 13. *Post hoc* tests were Tukey corrected for multiple comparison. Differences were

804 considered significant for $p < 0.05$.

805 ## 5.5 **MRI data acquisition**

806 The birds were initially anesthetized using 2% Isoflurane (Isoflo ®, Abbot Laboratories Ltd.) in a mixture

807 of 30% O_2 and 70% N_2 at a flow rate of 600 ml/min. Throughout the entire imaging procedure,

808   respiration rate was monitored with a small pneumatic sensor (SA Instruments, NY, USA) positioned

809   under the bird. Depending on the breathing rate, the anesthetic dose was lowered, ranging between

810   1% - 2% isoflurane. Body temperature was monitored with a cloacal temperature probe and kept

811   within narrow physiological ranges (41.0 ± 0.2 °C) using a warm air system with a feedback unit (SA

812   Instruments, NY, USA).

813   All MRI measurements were performed on a 7T horizontal MR system (Pharmascan 70/16 US, Bruker

814   Biospin, Germany). Each imaging session started with a T2-weighted 3D anatomical RARE scan (TR:

815   2000 ms; TE: 11 ms; RARE factor: 8; zero-filled to a matrix of (256x92x64) with voxel resolution

816   (0.089x0.25x0.25) mm³). Subsequently, a 4 shot SE-EPI DTI scan (TR: 7000 ms; TE: 23 ms; d 4ms, D

817   12ms; b-value 670 s/mm²; 60 diffusion gradient directions; spatial resolution: (0.179x0.179x0.35)

818   mm³; 28 coronal slices) was acquired. After the imaging procedure, birds were left to recover in a

819   warmed recovery box before returning to the aviary.

820   ## 5.6 MRI data processing

821   Diffusion data was analyzed with the Diffusion II toolbox in SPM12 software (Statistical Parametric

822   Mapping, http://www.fil.ion.ucl.ac.uk/spm/software/spm12/). In a first step, the diffusion weighted

823   (DW) images were realigned to correct for motion, using a rigid registration between the b0 images.

824   This motion correction was then extended to all DW-images. Next, the realigned DW-images were co-

825   registered to the anatomical 3D image of each subject using normalized mutual information as the

826   similarity metric. Earlier a 3D template was created from all the subject anatomical 3D scans using

827   ANTs (Advanced Normalization Tools)(Avants, Yushkevich et al. 2010), providing a standardized

828   neuroanatomical space of the female starling brain. This facilitated normalization of the individual 3D

829   images to the template. The normalization parameters from the 3D images were applied to the co-

830   registered DW-images. Subsequently, the diffusion information was reoriented to correct for changes

831   due to realignment, co-registration and normalization. Diffusion tensor was estimated from the DW-

832   data and DTI parameter maps were derived (i.e. fractional anisotropy (FA), mean diffusivity (MD),

833   eigenvalue 1 (λ1) or axonal diffusivity and radial diffusivity (RD, mean of λ2 & λ3) maps). Finally, all DTI

834   parameter maps were smoothed using a Gaussian kernel of double the voxel size (FWHM= 0.36 x 0.36

835   x 0.48 mm³). After every processing step, images were checked for errors due to excessive motion,

836   failed normalization or distortions. Outliers were removed from further processing.

5.7 **Statistical analysis DTI**

The normalized DTI parameter maps were used for voxel based analysis and ROI based analysis. The voxel based analysis included one way ANOVA to look for significant changes over time and multiple regression to investigate correlations to song behavior and testosterone. We performed these analyses with a whole brain mask and subsequently with a mask for song control nuclei, auditory system and their tracts. This way we ensured not to miss significant changes in relevant regions that might be obscured by the stringent correction for multiple comparisons in whole brain analysis.

ROI's defined on the starling atlas (De Groof, George et al. 2016) were transformed to match the template space. Using the MarsBaR toolbox of SPM, mean DTI values could be extracted from the different ROI's in automated way for a normalized ROI based analysis (Brett, Anton et al. 2002).

In addition, individual DTI parameter maps were reconstructed without normalization to the template, so that changes in volume were not obscured by normalization. Using the neuroanatomical contrast of the fractional anisotropy maps we could delineate different ROI's (telencephalon, RA and HVC-RA tract) using AMIRA software (De Groof, Verhoye et al. 2006). This way we could determine volume and DTI changes within these ROI's. Linear mixed model with *post hoc* Tukey correction was performed on the ROI data using JMP Pro 13. Differences were considered significant for p<0.05.

853   6.   # Supplementary information

854
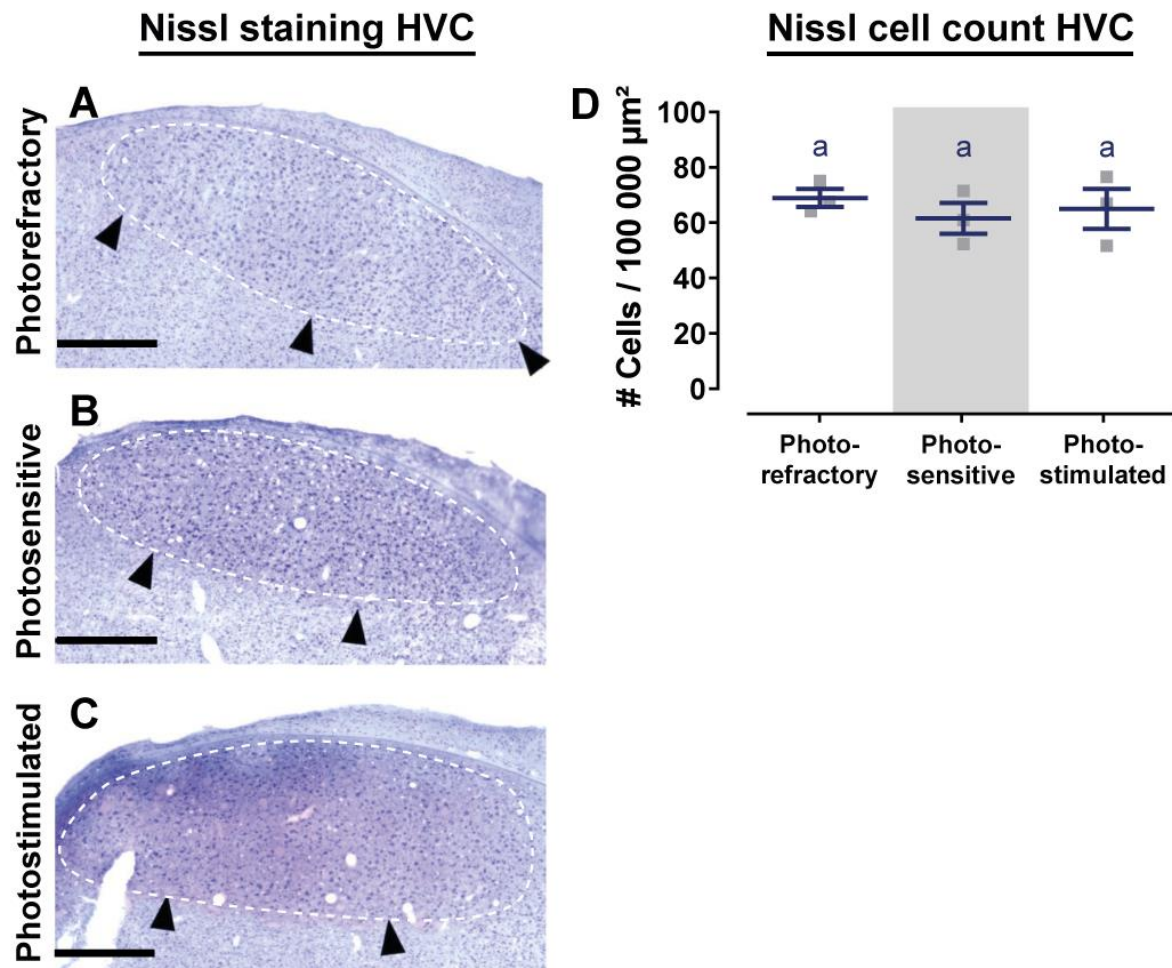
Figure 3 – figure supplement 1: Representative images of the HVC of starlings in different photoperiodic states stained by cresyl violet (A, B, C) and quantitative analysis of the Nissl cell count in the HVC. The border of HVC is designated by white dashed lines and black arrowheads. Scale bar = 500 μm. Horizontal bars represent the average with standard deviation error bars (n=3). The grey area indicates the photosensitive phase.
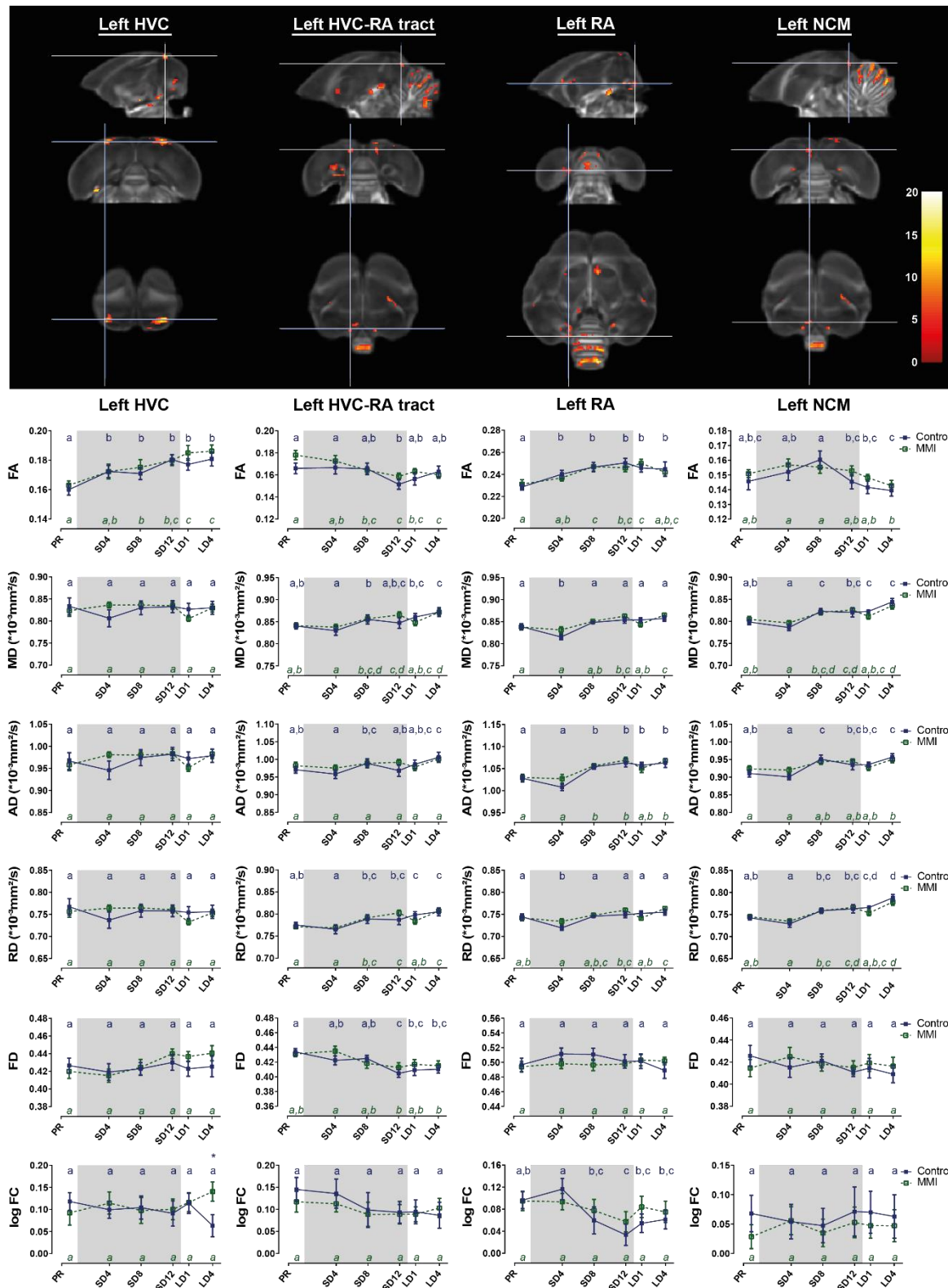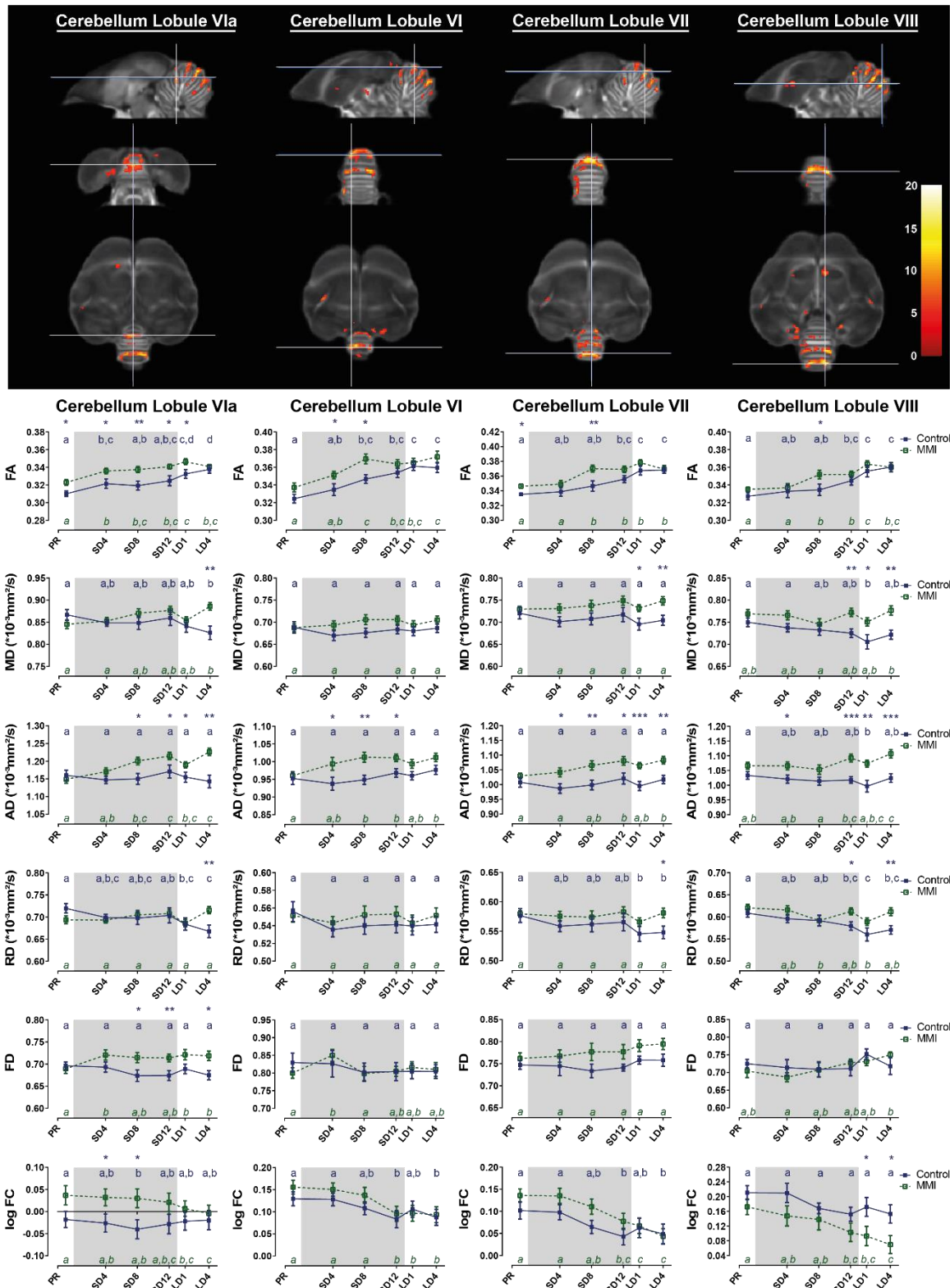
Figure 6 – figure supplement 1: Summary of the significant longitudinal changes over time in FA, MD, AD, RD, FD and log FC extracted from ROI-based clusters at level of the left HVC, HVC-RA tract, RA and NCM.

863
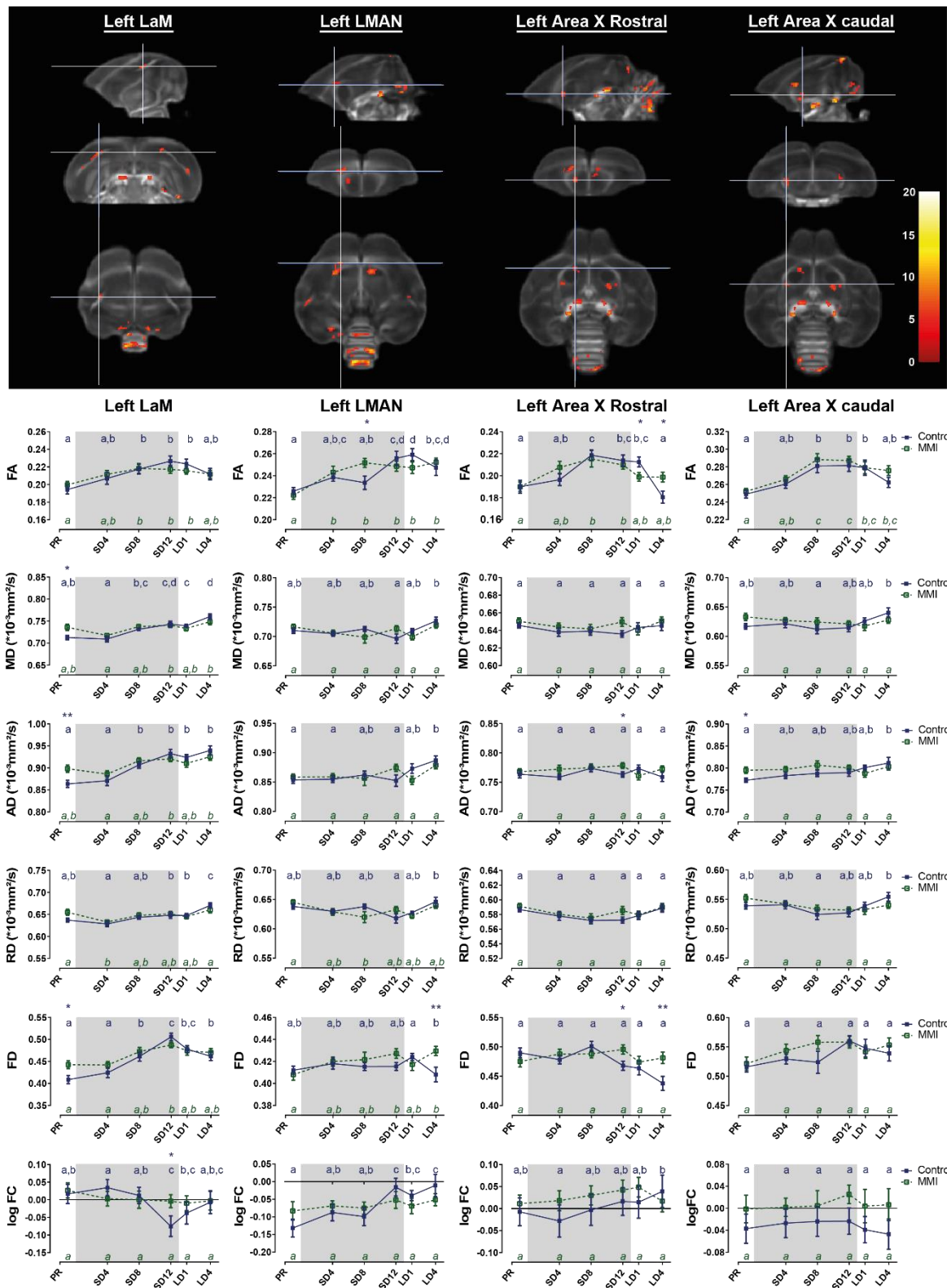
Figure 6 – figure supplement 2: Summary of the significant longitudinal changes over time in FA, MD, AD, RD, FD and log FC extracted from ROI-based clusters at level of the left LaM, LMAN, Area X rostral and caudal surroundings.
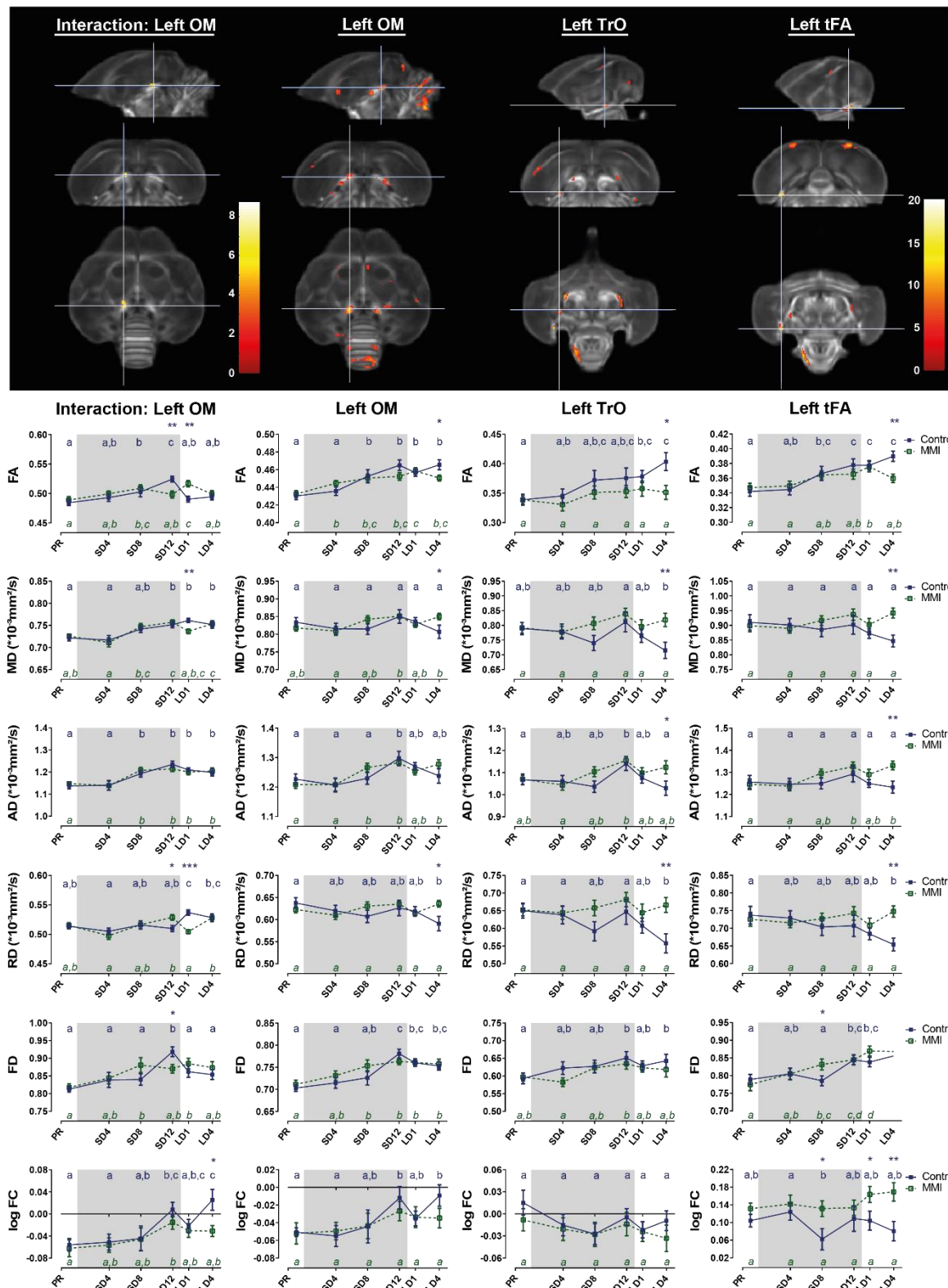
Figure 7 – figure supplement 1: Summary of the significant longitudinal changes over time in FA, MD, AD, RD, FD and log FC extracted from ROI-based clusters at level of the left OM, TrO and tFA.

870

Figure 7 – figure supplement 1: : Summary of the significant longitudinal changes over time in FA, MD, AD, RD, FD and log FC extracted from ROI-based clusters at level of the cerebellar lobules VIa, VI, VII and VIII.

873 7. # Acknowledgements

880 8.   # References

881   Alward, B. A., J. Balthazart and G. F. Ball (2013). "Differential effects of global versus local testosterone
882   on singing behavior and its underlying neural substrate." Proc Natl Acad Sci U S A **110**(48): 19573-
883   19578.
884   Alward, B. A., J. Balthazart and G. F. Ball (2017). "Dissociable Effects on Birdsong of Androgen Signaling
885   in Cortex-Like Brain Regions of Canaries." J Neurosci **37**(36): 8612-8624.
886   Alward, B. A., W. D. Mayes, K. Peng, T. J. Stevenson, J. Balthazart and G. F. Ball (2014). "Dissociable
887   effects of social context on song and doublecortin immunoreactivity in male canaries." Eur J Neurosci
888   **40**(6): 2941-2947.
889   Avants, B. B., P. Yushkevich, J. Pluta, D. Minkoff, M. Korczykowski, J. Detre and J. C. Gee (2010). "The
890   optimal template effect in hippocampus studies of diseased populations." Neuroimage **49**(3): 2457-
891   2466.
892   Ball, G. F. and J. C. Wingfield (1987). "Changes in Plasma Levels of Luteinizing Hormone and Sex Steroid
893   Hormones in Relation to Multiple-Broodedness and Nest-Site Density in Male Starlings." Physiological
894   Zoology **60**(2): 191-199.
895   Balmer, T. S., V. M. Carels, J. L. Frisch and T. A. Nick (2009). "Modulation of Perineuronal Nets and
896   Parvalbumin with Developmental Song Learning." The Journal of Neuroscience **29**(41): 12878-12885.
897   Balthazart, J., T. D. Charlier, J. M. Barker, T. Yamamura and G. F. Ball (2010). "Sex steroid-induced
898   neuroplasticity and behavioral activation in birds." Eur J Neurosci **32**(12): 2116-2132.
899   Batista, G. and T. K. Hensch (2019). "Critical Period Regulation by Thyroid Hormones: Potential
900   Mechanisms and Sex-Specific Aspects." Front Mol Neurosci **12**: 77.
901   Bentley, G. E., A. Dawson and A. R. Goldsmith (2000). "Lack of gonadotrophin-releasing hormone
902   (GnRH) neuron response to decreasing photoperiod in thyroidectomized male starlings (Sturnus
903   vulgaris)." Journal of Experimental Zoology **287**(1): 74-79.
904   Bentley, G. E., A. R. Goldsmith, A. Dawson, L. M. Glennie, R. T. Talbot and P. J. Sharp (1997).
905   "Photorefractoriness in European starlings (Sturnus vulgaris) is not dependent upon the long-day-
906   induced rise in plasma thyroxine." General and Comparative Endocrinology **107**(3): 428-438.
907   Bentley, G. E., S. Tucker, H. Chou, M. Hau and N. Perfito (2013). "Testicular growth and regression are
908   not correlated with Dio2 expression in a wild male songbird, sturnus vulgaris, exposed to natural
909   changes in photoperiod." Endocrinology **154**(5): 1813-1819.
910   Bentley, G. E., T. J. Van't Hof and G. F. Ball (1999). "Seasonal neuroplasticity in the songbird
911   telencephalon: A role for melatonin." Proceedings of the National Academy of Sciences of the United
912   States of America **96**(8): 4674-4679.
913   Bernal, J. (2000). Thyroid Hormones in Brain Development and Function. Endotext. K. R. Feingold, B.
914   Anawalt, A. Boyce et al. South Dartmouth (MA), MDText.com, Inc.
915   Copyright © 2000-2020, MDText.com, Inc.
916   Bernard, D. J., G. E. Bentley, J. Balthazart, F. W. Turek and G. F. Ball (1999). "Androgen receptor,
917   estrogen receptor alpha, and estrogen receptor beta show distinct patterns of expression in forebrain
918   song control nuclei of European starlings." Endocrinology **140**(10): 4633-4643.
919   Bernard, D. J., M. Eens and G. F. Ball (1996). "Age- and behavior-related variation in volumes of song
920   control nuclei in male European starlings." J Neurobiol **30**(3): 329-339.
921   Bourgeois, N. M., S. L. Van Herck, P. Vancamp, J. Delbaere, C. Zevenbergen, S. Kersseboom, V. M.
922   Darras and T. J. Visser (2016). "Characterization of Chicken Thyroid Hormone Transporters."
923   Endocrinology **157**(6): 2560-2574.
924   Bradley, D. J., H. C. Towle and W. S. r. Young (1992). "Spatial and temporal expression of alpha- and
925   beta-thyroid hormone receptor mRNAs, including the beta 2-subtype, in the developing mammalian
926   nervous system." J Neurosci **12**(6): 2288-2302.

Brett, M., J. Anton, R. Valabregue and J. Poline (2002). Region of interest analysis using an SPM toolbox. 8th International Conference on Functional Mapping of the Human Brain, Sendai, Japan.

Caro, S. P., M. M. Lambrechts and J. Balthazart (2005). "Early seasonal development of brain song control nuclei in male blue tits." Neuroscience Letters **386**: 139-144.

Cornez, G., C. Collignon, W. Müller, G. F. Ball, C. A. Cornil and J. Balthazart (2020). "Seasonal changes of perineuronal nets and song learning in adult canaries (Serinus canaria)." Behavioural Brain Research **380**: 112437.

Cornez, G., F. N. Madison, A. Van der Linden, C. Cornil, K. M. Yoder, G. F. Ball and J. Balthazart (2017). "Perineuronal nets and vocal plasticity in songbirds: A proposed mechanism to explain the difference between closed-ended and open-ended learning." Dev Neurobiol **77**(8): 975-994.

Darras, V. M., S. L. Van Herck, M. Heijlen and B. De Groef (2011). "Thyroid hormone receptors in two model species for vertebrate embryonic development: chicken and zebrafish." J Thyroid Res **2011**: 402320.

Dawson, A., A. R. Goldsmith and T. J. Nicholls (1985). "Thyroidectomy results in termination of photorefractoriness in starlings (Sturnus vulgaris) kept in long daylengths." J Reprod Fertil **74**(2): 527-533.

Dawson, A., A. R. Goldsmith, T. J. Nicholls and B. K. Follett (1986). "Endocrine changes associated with the termination of photorefractoriness by short daylengths and thyroidectomy in starlings (Sturnus vulgaris)." J Endocrinol **110**(1): 73-79.

Dawson, A., V. M. King, G. E. Bentley and G. F. Ball (2001). "Photoperiodic control of seasonality in birds." J Biol Rhythms **16**(4): 365-380.

De Groof, G., I. George, S. Touj, M. Stacho, E. Jonckers, H. Cousillas, M. Hausberger, O. Gunturkun and A. Van der Linden (2016). "A three-dimensional digital atlas of the starling brain." Brain Struct Funct **221**(4): 1899-1909.

De Groof, G., M. Verhoye, V. Van Meir, I. Tindemans, A. Leemans and A. Van der Linden (2006). "In vivo diffusion tensor imaging (DTI) of brain subdivisions and vocal pathways in songbirds." Neuroimage **29**(3): 754-763.

Eens, M. (1997). "Understanding the Complex Song of the European Starling: An Integrated Ethological Approach." **26**: 355-434.

Forrest, D., F. Hallböök, H. Persson and B. Vennström (1991). "Distinct functions for thyroid hormone receptors alpha and beta in brain development indicated by differential expression of receptor genes." EMBO J **10**(2): 269-275.

Fusani, L., T. J. Van't Hof, J. B. Hutchison and M. Gahr (2000). "Seasonal expression of androgen receptors, estrogen receptors, and aromatase in the canary brain in relation to circulating androgens and estrogens." J Neurobiol **43**: 254-268.

Gahr, M. (1990). "Localization of androgen receptors and estrogen receptors in the same cells of the songbird brain." Proc Natl Acad Sci U S A **87**: 9445-9448.

Gahr, M. and R. Metzdorf (1997). "Distribution and dynamics in the expression of androgen and estrogen receptors in vocal control systems of songbirds." Brain Res Bull **44**(4): 509-517.

Garamszegi, L. Z. and M. Eens (2004). "Brain space for a learned task: strong intraspecific evidence for neural correlates of singing behavior in songbirds." Brain Res Brain Res Rev **44**(2-3): 187-193.

Gereben, B., A. M. Zavacki, S. Ribich, B. W. Kim, S. A. Huang, W. S. Simonides, A. Zeöld and A. C. Bianco (2008). "Cellular and molecular basis of deiodinase-regulated thyroid hormone signaling." Endocrine reviews **29**(7): 898-938.

Gil-Ibanez, P., F. Garcia-Garcia, J. Dopazo, J. Bernal and B. Morte (2017). "Global Transcriptome Analysis of Primary Cerebrocortical Cells: Identification of Genes Regulated by Triiodothyronine in Specific Cell Types." Cereb Cortex **27**(1): 706-717.

Guadaño-Ferraz, A., M. J. Escámez, E. Rausell and J. Bernal (1999). "Expression of type 2 iodothyronine deiodinase in hypothyroid rat brain indicates an important role of thyroid hormone in the development of specific primary sensory systems." The Journal of neuroscience : the official journal of the Society for Neuroscience **19**(9): 3430-3439.

978 Hamaide, J., K. Lukacova, J. Orije, G. A. Keliris, M. Verhoye and A. Van der Linden (2020). "In vivo
979 assessment of the neural substrate linked with vocal imitation accuracy." Elife **9**.

980 Harsan, L. A., J. Steibel, A. Zaremba, A. Agin, R. Sapin, P. Poulet, B. Guignard, N. Parizel, D. Grucker, N.
981 Boehm, R. H. Miller and M. S. Ghandour (2008). "Recovery from chronic demyelination by thyroid
982 hormone therapy: myelinogenesis induction and assessment by diffusion tensor magnetic resonance
983 imaging." J Neurosci **28**(52): 14189-14201.

984 Heuer, H. and T. J. Visser (2009). "Pathophysiological Importance of Thyroid Hormone Transporters."
985 Endocrinology **150**(3): 1078-1083.

986 Korsia, S. and S. W. Bottjer (1991). "Chronic testosterone treatment impairs vocal learning in male
987 zebra finches during a restricted period of development." The Journal of neuroscience : the official
988 journal of the Society for Neuroscience **11**(8): 2362-2371.

989 Lim, W., N. H. Nguyen, H. Y. Yang, T. S. Scanlan and J. D. Furlow (2002). "A thyroid hormone antagonist
990 that inhibits thyroid hormone action in vivo." J Biol Chem **277**(38): 35664-35670.

991 Marler, P., S. Peters, G. F. Ball, A. M. Dufty, Jr. and J. C. Wingfield (1988). "The role of sex steroids in
992 the acquisition and production of birdsong." Nature **336**(6201): 770-772.

993 Merullo, D. P., M. A. Cordes, S. A. Stevenson and L. V. Riters (2015). "Neurotensin immunolabeling
994 relates to sexually-motivated song and other social behaviors in male European starlings (Sturnus
995 vulgaris)." Behav Brain Res **282**: 133-143.

996 Metzdorf, R., M. Gahr and L. Fusani (1999). "Distribution of aromatase, estrogen receptor, and
997 androgen receptor mRNA in forebrain of songbirds and nonsongbirds." J Comp Neurol **407**: 15.

998 Nakao, N., H. Ono, T. Yamamura, T. Anraku, T. Takagi, K. Higashi, S. Yasuo, Y. Katou, S. Kageyama, Y.
999 Uno, T. Kasukawa, M. Iigo, P. J. Sharp, A. Iwasawa, Y. Suzuki, S. Sugano, T. Niimi, M. Mizutani, T.
1000 Namikawa, S. Ebihara, H. R. Ueda and T. Yoshimura (2008). "Thyrotrophin in the pars tuberalis triggers
1001 photoperiodic response." Nature **452**(7185): 317-322.

1002 Nicholls, T. J., A. R. Goldsmith and A. Dawson (1988). "Photorefractoriness in birds and comparison
1003 with mammals." Physiological Reviews **68**(1): 133-176.

1004 Nicholson, D. A., T. F. Roberts and S. J. Sober (2018). "Thalamostriatal and cerebellothalamic pathways
1005 in a songbird, the Bengalese finch." J Comp Neurol **526**(9): 1550-1570.

1006 Nottebohm, F., M. E. Nottebohm, L. A. Crane and J. C. Wingfield (1987). "Seasonal changes in gonadal
1007 hormone levels of adult male canaries and their relation to song." Behavioral and Neural Biology **47**(2):
1008 197-211.

1009 Orije, J., E. Cardon, G. de Groof, J. Hamaide, E. Jonckers, S. Van Massenhoven, V. Darras, J. Balthazart,
1010 M. Verhoye and A. Van der Linden (2020). "In vivo online monitoring of testosterone-induced
1011 neuroplasticity in a female songbird." Horm Behav **118**.

1012 Orije, J., E. Cardon, J. Hamaide, E. Jonckers, V. M. Darras, M. Verhoye and A. Van der Linden (2021).
1013 "The photosensitive phase acts as a sensitive window for seasonal multisensory neuroplasticity in
1014 male and female starlings." bioRxiv: 2021.2001.2021.427111.

1015 Orije, J., E. Cardon, J. Hamaide, E. Jonckers, V. M. Darras, M. Verhoye and A. Van der Linden (2021).
1016 "Uncovering a 'sensitive window' of multisensory and motor neuroplasticity in the cerebrum and
1017 cerebellum of male and female starlings." Elife **10**.

1018 Pant, K. and A. Chandola-Saklani (1993). "Effects of thyroxine on avian moulting may not involve prior
1019 conversion to tri-iodothyronine." J Endocrinol **137**(2): 265-270.

1020 Pérez, J. H., S. L. Meddle, J. C. Wingfield and M. Ramenofsky (2018). "Effects of thyroid hormone
1021 manipulation on pre-nuptial molt, luteinizing hormone and testicular growth in male white-crowned
1022 sparrows (Zonotrichia leuchophrys gambelii)." General and Comparative Endocrinology **255**: 12-18.

1023 Person, A. L., S. D. Gale, M. A. Farries and D. J. Perkel (2008). "Organization of the songbird basal
1024 ganglia, including area X." J Comp Neurol **508**(5): 840-866.

1025 Pidoux, L., P. Le Blanc, C. Levenes and A. Leblois (2018). "A subcortical circuit linking the cerebellum
1026 to the basal ganglia engaged in vocal learning." Elife **7**.

1027 Raparti, G., S. Jain, K. Ramteke, M. Murthy, R. Ghanghas, S. Ramanand and J. Ramanand (2013).
1028 "Selective thyroid hormone receptor modulators." Indian journal of endocrinology and metabolism
1029 **17**(2): 211-218.
1030 Raymaekers, S. R., W. Verbeure, S. M. Ter Haar, C. A. Cornil, J. Balthazart and V. M. Darras (2017). "A
1031 dynamic, sex-specific expression pattern of genes regulating thyroid hormone action in the developing
1032 zebra finch song control system." Gen Comp Endocrinol **240**: 91-102.
1033 Reyns, G. E., K. A. Janssens, J. Buyse, E. R. Kühn and V. M. Darras (2002). "Changes in thyroid hormone
1034 levels in chicken liver during fasting and refeeding." Comp Biochem Physiol B Biochem Mol Biol **132**(1):
1035 239-245.
1036 Riters, L. V., M. Baillien, M. Eens, R. Pinxten, A. Foidart, G. F. Ball and J. Balthazart (2001). "Seasonal
1037 Variation in Androgen-Metabolizing Enzymes in the Diencephalon and Telencephalon of the Male
1038 European Starling (Sturnus vulgaris)." J Neuroendocrinol **13**(11): 985-997.
1039 Riters, L. V., M. Eens, R. Pinxten and G. F. Ball (2002). "Seasonal changes in the densities of alpha(2)
1040 noradrenergic receptors are inversely related to changes in testosterone and the volumes of song
1041 control nuclei in male European starlings." J Comp Neurol **444**(1): 63-74.
1042 Rouse, M. L., Jr., T. J. Stevenson, E. S. Fortune and G. F. Ball (2015). "Reproductive state modulates
1043 testosterone-induced singing in adult female European starlings (Sturnus vulgaris)." Horm Behav **72**:
1044 78-87.
1045 Shevchouk, O. T., G. F. Ball, C. A. Cornil and J. Balthazart (2017). "Studies of HVC Plasticity in Adult
1046 Canaries Reveal Social Effects and Sex Differences as Well as Limitations of Multiple Markers Available
1047 to Assess Adult Neurogenesis." PLoS One **12**(1): e0170938.
1048 Smith, G. T., E. A. Brenowitz and J. C. Wingfield (1997). "Roles of photoperiod and testosterone in
1049 seasonal plasticity of the avian song control system." Journal of Neurobiology **32**(4): 426-442.
1050 Stevenson, T. J., K. Replogle, J. Drnevich, D. F. Clayton and G. F. Ball (2012). "High throughput analysis
1051 reveals dissociable gene expression profiles in two independent neural systems involved in the
1052 regulation of social behavior." BMC Neurosci **13**: 126.
1053 Thompson, C. K., J. Meitzen, K. Replogle, J. Drnevich, K. L. Lent, A. M. Wissman, F. M. Farin, T. K.
1054 Bammler, R. P. Beyer, D. F. Clayton, D. J. Perkel and E. A. Brenowitz (2012). "Seasonal changes in
1055 patterns of gene expression in avian song control brain regions." PLoS One **7**(4): e35119.
1056 Tramontin, A. D., N. Perfito, J. C. Wingfield and E. A. Brenowitz (2001). "Seasonal Growth of Song
1057 Control Nuclei Precedes Seasonal Reproductive Development in Wild Adult Song Sparrows." General
1058 and Comparative Endocrinology **122**(1): 1-9.
1059 Tramontin, A. D., J. C. Wingfield and E. A. Brenowitz (1999). "Contributions of social cues and
1060 photoperiod to seasonal plasticity in the adult avian song control system." J Neurosci **19**(1): 476-483.
1061 Valle, L. B., R. M. Oliveira-Filho, J. H. Romaldini and P. F. Lara (1985). "Pituitary-testicular axis
1062 abnormalities in immature male hypothyroid rats." J Steroid Biochem **23**(3): 253-257.
1063 Van Herck, S. L., J. Delbaere, N. M. Bourgeois, B. M. McAllan, S. J. Richardson and V. M. Darras (2015).
1064 "Expression of thyroid hormone transporters and deiodinases at the brain barriers in the embryonic
1065 chicken: Insights into the regulation of thyroid hormone availability during neurodevelopment." Gen
1066 Comp Endocrinol **214**: 30-39.
1067 Van Herck, S. L., S. Geysens, J. Delbaere and V. M. Darras (2013). "Regulators of thyroid hormone
1068 availability and action in embryonic chicken brain development." Gen Comp Endocrinol **190**: 96-104.
1069 Van Hout, A. J., M. Eens, V. M. Darras and R. Pinxten (2010). "Acute stress induces a rapid increase of
1070 testosterone in a songbird: implications for plasma testosterone sampling." Gen Comp Endocrinol
1071 **168**(3): 505-510.
1072 Van Hout, A. J., R. Pinxten, V. M. Darras and M. Eens (2012). "Testosterone increases repertoire size
1073 in an open-ended learner: an experimental study using adult male European starlings (Sturnus
1074 vulgaris)." Horm Behav **62**(5): 563-568.
1075 Voigt, C. and S. Leitner (2008). "Seasonality in song behaviour revisited: seasonal and annual variants
1076 and invariants in the song of the domesticated canary (Serinus canaria)." Horm Behav **54**(3): 373-378.

1077   Wang, S., C. Liao, F. Li, S. Liu, W. Meng and D. Li (2014). "Castration modulates singing patterns and
1078   electrophysiological properties of RA projection neurons in adult male zebra finches." PeerJ **2**: e352-
1079   e352.
1080   Watanabe, T., T. Yamamura, M. Watanabe, S. Yasuo, N. Nakao, A. Dawson, S. Ebihara and T. Yoshimura
1081   (2007). "Hypothalamic expression of thyroid hormone-activating and -inactivating enzyme genes in
1082   relation to photorefractoriness in birds and mammals." American Journal of Physiology-Regulatory
1083   Integrative and Comparative Physiology **292**(1): R568-R572.
1084   Weng, Q., E. Saita, G. Watanabe, S. Takahashi, M. Sedqyar, A. K. Suzuki, S. Taneda and K. Taya (2007).
1085   "Effect of methimazole-induced hypothyroidism on adrenal and gonadal functions in male Japanese
1086   quail (Coturnix japonica)." J Reprod Dev **53**(6): 1335-1341.
1087   Williams, H., D. M. Connor and J. W. Hill (2003). "Testosterone decreases the potential for song
1088   plasticity in adult male zebra finches." Hormones and Behavior **44**(5): 402-412.
1089   Wingfield, J. C. and B. Silverin (2002). Ecophysiological studies of hormone behavior relations in birds
1090   Hormones, brain and behavior. D. W. Pfaff**:** 587-647.
1091   Yamaguchi, S., N. Aoki, T. Kitajima, E. Iikubo, S. Katagiri, T. Matsushima and K. J. Homma (2012).
1092   "Thyroid hormone determines the start of the sensitive period of imprinting and primes later
1093   learning." Nat Commun **3**: 1081.
1094   Yoshihara, H. A. and T. S. Scanlan (2003). "Selective thyroid hormone receptor modulators." Curr Top
1095   Med Chem **3**(14): 1601-1616.
1096   Yoshimura, T. (2013). "Thyroid hormone and seasonal regulation of reproduction." Front
1097   Neuroendocrinol **34**(3): 157-166.
1098   Yoshimura, T., S. Yasuo, M. Watanabe, M. Iigo, T. Yamamura, K. Hirunagi and S. Ebihara (2003). "Light-
1099   induced hormone conversion of T-4 to T-3 regulates photoperiodic response of gonads in birds."
1100   Nature **426**(6963): 178-181.
1101   Yoshimura, T., S. Yasuo, M. Watanaben, M. Iigo, T. Yamamura, K. Hirunagi and S. Ebihara (2003).
1102   "Light-induced hormone conversion of T4 to T3 regulates photoperiodic response of gonads in birds."
1103   Nature **426**(6963): 178-181.
1104